Untargeted metabolomics of neuronal cell culture: A model system for the toxicity testing of insecticide chemical exposure

Short title

Cell metabolomics in neurotoxicity of insecticides

Authors

Sarah Hayton [1,2], Garth L Maker [1,2], Ian Mullaney [2] and Robert D Trengove [1].

[1] Separation Sciences and Metabolomics Laboratories, Murdoch University, Perth, Western Australia.

[2] School of Veterinary and Life Sciences, Murdoch University, Perth, Western Australia.

Corresponding author

Dr. Garth L Maker

Medical and Molecular Sciences
School of Veterinary and Life Sciences
Murdoch University
South Street
Murdoch
6150
Western Australia

Phone: 61 8 9360 1288
Fax: 61 8 9360 1240
G.Maker@murdoch.edu.au

Keywords

Permethrin; Malathion; neurotoxicity; B50 cell line; metabolomics; GC-MS

Sponsors

This work was supported in part by the National Collaborative Research Infrastructure Strategy Bioplatforms Australia, the Australian Government Research Training Program Scholarship, and the McCusker Charitable Foundation.

Standard Abstract

Toxicity testing is essential for the protection of human health from exposure to toxic environmental chemicals. As traditional toxicity testing is carried out using animal models, mammalian cell culture models are becoming an increasingly attractive alternative to animal testing. Combining the use of mammalian cell culture models with screening-style molecular profiling technologies, such as metabolomics, can uncover previously unknown biochemical bases of toxicity. We have used a mass spectrometry-based untargeted metabolomics approach to characterise for the first time the changes in the metabolome of the B50 cell line, an immortalised rat neuronal cell line, following acute exposure to two known neurotoxic chemicals that are common environmental contaminants; the pyrethroid insecticide permethrin and the organophosphate insecticide malathion. B50 cells were exposed to either the dosing vehicle (methanol) or an acute dose of either permethrin or malathion for 6 and 24 hours. Intracellular metabolites were profiled by gas chromatography-mass spectrometry. Using Principal Component Analysis, we selected the key metabolites whose abundance was altered by chemical exposure. By considering the major fold changes in abundance (>2.0 or <0.5 from control) across these metabolites, we were able to elucidate important cellular events associated with toxic exposure including disrupted energy metabolism and attempted protective mechanisms from excitotoxicity. Our findings illustrate the ability of mammalian cell culture metabolomics to detect finer metabolic effects of acute exposure to known toxic chemicals, and validates the need for further development of this process in the application of trace-level dose and chronic toxicity studies, and toxicity testing of unknown chemicals.

Short Abstract

The use of mammalian cell culture models combined with powerful molecular profiling techniques can uncover unknown biochemical bases of toxicity and provide an alternative to toxicity testing in animals. An untargeted metabolomics approach was used to characterise the metabolome of B50 rat neuronal cells, following exposure to two neurotoxic insecticides, permethrin and malathion. Cells were profiled by gas chromatography-mass spectrometry. A number of key intracellular metabolites were identified and important cellular events including energy metabolism were disrupted by chemical exposure.

Introduction

Insecticides have been used across the globe for several decades as the forefront of efforts to control pest species that threaten agriculture, animal or human health. The use of insecticides has allowed for greater human access to farmed food, strengthened agricultural economies, and prevented outbreaks in vector-borne diseases such as malaria (Curtis and Mnzava 2000, Hemingway 2014). As the use of insecticides is widespread, and knowledge of their persistence in the environment is uncovered, there is growing concern about their use and the implications of human exposure (Fragar et al 2005). Insecticide chemicals are known neurotoxins and elicit their effects on the target species by targeting features of the insect nervous system. Unfortunately, there are many features of the nervous system which are conserved across all animal species, and so insecticides can exert their toxic effects on non-target species (Keifer and Firestone 2007).

Human exposure to insecticides has been associated with a range of neuronal health concerns, such as the prevalence of Alzheimer's Disease (Welsh-Bohmer et al 2010, Zaganas et al 2013), Parkinson's Disease (Ascherio et al 2006, Moretto and Colosio 2011), and in childhood brain tumours (Searles Nielson et al 2010), neurodevelopment (Lee et al 2015) and associated disorders such as Attention-Deficit-Hyperactivity Disorder and Autism Spectrum Disorders (Bouchard et al 2010, Flaskos 2012, Liu and Schelar 2012, Roberts et al 2007, Timofeeva and Levin 2010). Many insecticide chemicals are lipophilic, meaning they can accumulate within fat stores in the body and have access to the nervous system by crossing the blood-brain barrier (Egan 1966, Kohlmeier and Kohlmeier 1995, Maroni et al 2000). A number of recent studies have investigated the presence of insecticides and their metabolites in young children from both rural and urban areas in the United States, Europe and Australia (Babina et al 2012, Becker et al 2006, Fenske et al 2002, Heudorf et al 2004, Lu et al 2009, Naeher et al 2010), indicating not only the widespread exposure of insecticides and their potential for bioaccumulation, but also their potential bioavailability during key stages of development in children.

Current knowledge of the long-term human toxicity of insecticides tends to focus on the physiological end-points of exposure, often making assumptions by association. Despite the varied, specific molecular targets of the different insecticide chemical classes, the overall intended effect of insecticides on the cells of the nervous system is the same: the initial over-stimulation and excitation of neuronal cells, resulting in cell exhaustion, degeneration and death (Marrs 2012, Narahashi 2010). The specific molecular targets, or mechanisms of toxic action are well known throughout the many different classes of insecticide chemicals, as they have been elucidated from traditional toxicity testing on animals and through the development of new chemical compounds that are similar in structure and thus have the same targets as their parent compound (Stenersen 2004). What remains unknown about the toxicity of insecticides are the immediate metabolic effects of these chemicals on the processes that occur inside neuronal cells, and what these might mean for the prolonged health of the cell and thus the nervous system. Understanding these small metabolic perturbations in neuronal cells that survive a toxic insult could potentially uncover some of the specific biochemical process that may be responsible for the adverse effects on human health associated with insecticide chemical exposure.

Metabolite profiling (metabolomics/metabonomics) provides unique insights into the metabolic pathways of cells via the simultaneous, untargeted analysis of the small molecules

(or metabolites) within a biological sample. Metabolomics has been widely applied in the field of toxicology, mainly in the context of animal studies and the analysis of urine or plasma for the discovery of biomarkers of toxic chemical exposure (Bouhifd et al 2013, Ramirez et al 2013). There are studies that have utilised mammalian cell culture metabolomics to look specifically at the metabolic effects of toxic chemical exposure (Ellis et al 2011, Huang et al 2012, Johnson et al 2012, Snouber et al 2013, Van den Hof et al 2015), only a handful of these have specifically investigated neurotoxicity (Zurich and Monnet-Tschudi 2009) including exposure to thalidomide (Qin et al 2012), methyl-mercury and caffeine (van Vliet et al 2008). There is clearly great potential in the application of mammalian cell culture metabolomics in the study of insecticide toxicology, and metabolomics has been suggested to be an important technique in the development of new, safer pesticide chemicals (Aliferis and Chrysayi-Tokousbalides 2011).

The B50 neuroblastoma cell line was derived from the rat neonatal central nervous system (CNS) and is in wide use today in studies of CNS neurons in culture (Otey et al 2003). B50 cells have been used extensively to study neuronal cell death and neurotoxicity, and are very simple to grow, making them an ideal model to investigate the potential of metabolomics in the assessment of neurotoxicity. Before any cell line model can be used as a screening test for chemicals of unknown toxicity, it first has to be validated with chemicals of known toxic effect. In this study, we used gas chromatography-mass spectrometry (GC-MS)-based untargeted metabolomics to characterise the effects to the intracellular metabolome of the B50 neuronal cell line after 6 and 24 hours of acute exposure to two known neurotoxic chemicals: the pyrethroid insecticide permethrin (Soderlund 2012) and the organophosphate insecticide malathion (Flaskos 2012). Cell photographs were captured to compare metabolic response to any change in gross cell morphology. In particular, the main aim of this study was in showing that this metabolomic approach was able to identify significant fold changes in the metabolite profile of cultured mammalian neuronal cells following insult from a known toxic chemical. In addition, this study was also able to demonstrate how exposure to different classes of insecticides corresponded to distinctly different metabolite responses from the same cell line.

Materials and Methods

Cell culture

The adherent, rat neuroblastoma cell line B50 obtained from the European Collection of Cell Cultures (ECACC) was grown and maintained in Dulbecco's Modified Eagle Medium (DMEM) supplemented with 1% v/v 2 mM L-glutamine, 1% v/v 10,000 U/mL combined penicillin and streptomycin, and 5% v/v foetal calf serum (FCS). Cells were kept in a humidified incubator at 37^{o}C and 5% CO_2. Routine cell culture of adherent cell populations was performed in 75 cm^2 tissue culture flasks with 10 mL volume of medium during growth phase. Medium was replaced after 48 to 72 hours of initial seeding, when the phenol red indicator in the medium showed a drop in pH. For passaging confluent cells and cell counting during experimentation, cells were detached with addition of 0.25% Trypsin-EDTA solution (2.5g porcine trypsin and 0.2g EDTA per litre) after first removing the medium and washing the cells with pre-warmed 1 x phosphate-buffered saline (PBS). Cell culture passage numbers 28 to 32 were used for experimentation. The cells were tested using PCR for mycoplasma status along with HGH housekeeping gene and were found to be negative for presence of

mycoplasma. All cell culture solutions and PBS were purchased from Sigma-Aldrich (NSW, Australia).

Experimental design

For analysis of the metabolome, cells were cultivated in 6-well tissue culture plates and seeded at a density of 4 x 10^5 cells/well in 2 mL of medium. Plates were left for 24 hours to allow for cell adhesion before being exposed to either permethrin or malathion added as a solution in 100% methanol to a final concentration in each well of 200 µg/mL (equivalent to 0.51 and 0.61 mM for permethrin and malathion, respectively). Both compounds were purchased at the highest purity available (>98%, with permethrin as an equal mixture of *cis*- and *trans*-isomers) from Sigma-Aldrich. The final concentration of methanol in the cell medium was < 0.1% total volume. The same volume of methanol was added to the same number of equally prepared wells as an unexposed vehicle control group. Control and exposure groups for both time points of one insecticide exposure were set up simultaneously using cells from the same passage number to minimise uncontrolled variables. Five wells from one 6-well plate were combined as one sample within a particular treatment group. The sixth well was used to count the cell number as a representative parallel sample in order to normalise data to the amount of tissue analysed. The number of biological replicates set up per treatment group was four. Following addition of either insecticide compound, both 'non-exposed' and 'exposed' treatment groups for each compound were left for 6 hours and another set for 24 hours exposure, in a humidified incubator at 37°C and 5% CO_2. Immediately preceding sampling, cell number and viability were determined for each sample using Trypan blue exclusion following trypsinisation of the parallel cell number sample, by diluting 10 µL of cell suspension 1:2 with a 0.4% Trypan blue (Allied Chemicals; NSW, Australia) in 1 x PBS solution and immediately counting cells using a Bright-Line Haemocytometer (Hausser Scientific; PA, USA) and an inverted light microscope (Olympus Australia; VIC, Australia). Photographs were also taken immediately before sampling (Moticam 2300, Motic China Group Co.; Hong Kong) to document differences in cell density and gross morphology between control and exposure groups. All methanol and water used in this study was LC-MS-grade purity and purchased from LabScan (SA, Australia).

Sampling for intracellular metabolites

For analysis of intracellular metabolites, immediately following completion of the respective exposure time all plates of both unexposed and exposed treatment groups were removed from incubation and cellular activity halted by placing the plates directly onto ice. Culture medium was discarded and cellular metabolism immediately quenched by careful addition of 1 mL 4°C 1 x PBS to each well, ensuring minimal disruption of adhered cells from the plate surface. This PBS was removed as a washing step to remove any residual medium from the cells. Adhered cells were then collected by scraping into 100 µL of additional PBS and pooling the cell suspension from 5 wells into one microcentrifuge tube. All collected samples were immediately snap-frozen and freeze-dried using a FreeZone Plus Cascade Benchtop Freeze Dry System (Labconco; KO, USA) to prevent degradation or loss of metabolites (Mediani et al 2015). Freeze-dried samples were stored at -80°C until metabolite extraction.

For extraction of intracellular metabolites, freeze-dried cell samples were resuspended in 500 µL of 100% methanol containing 2.6 µg/mL of $^{13}C_6$-sorbitol (Sigma-Aldrich), an isotopically labelled compound that is easily resolved used as an internal standard to normalise analytical data, to minimise any observed effect from extraction or instrumental variability. The suspended cells in extraction solution were agitated in a Precellys 24 Tissue Lyser (Bertin Technologies; Aix-en-Provence, France) for 2 x 20 s cycles at 6,500 rpm to maximise the metabolite recovery rate. Homogenised extracts were centrifuged for 10 mins at 16,100 g and supernatant collected into fresh microcentrifuge tubes. Pellets of cell debris were discarded. Extracted metabolites were concentrated by evaporating the methanol in a Concentrator Plus Rotary Vacuum Concentrator (Eppendorf South Pacific; NSW, Australia) and protected from degradation by addition of water and further snap-freezing and freeze-drying. Once completely dry, metabolite extracts were stored at -80ºC until preparation for GC-MS analysis.

GC-MS analysis

For measurement of metabolites by GC-MS, dried metabolite extracts were derivatised by methoximation and silylation to increase thermal stability and volatility of metabolite compounds. The derivatisation process had been previously optimised for a range of different biological samples (Abbiss et al 2012, Abbiss et al 2015, Ng et al 2012, Wenner et al 2016). Briefly, 40 µL of 20 mg/mL methoxyamine hydrochloride in pyridine was added to a dried extract and incubated at 30ºC for 90 mins with agitation in a Thermomixer Comfort (Eppendorf) at 1,200 rpm, followed by addition of 20 µL of MSTFA (N-methyl-trimethylsilyltrifluoroacetamide) and incubation at 37ºC for 30 mins with agitation at 300 rpm. Derivatised metabolite extracts were transferred to amber vials with 200 µL glass inserts where 5 µL of *n*-alkanes mixture solubilised in hexane (C_{10} and C_{12} at 0.625 µg/mL and C_{15}, C_{19}, C_{22}, C_{26}, C_{32} and C_{36} at 1.250 µg/mL) was added to the sample to enable calculation of a Kovát's retention index. Derivatisation of samples was carried out in 'batches' to ensure that all derivatised samples were injected and analysed within 24 hours following derivatisation. Methoxyamine hydrochloride, MSTFA and *n*-alkanes were purchased from Sigma-Aldrich, pyridine from Ajax Finechem (NSW, Australia) and hexane from LabScan, all in the highest purity available.

A total of 1 µL of each sample was injected in splitless mode into a GC for compound separation, and mass separation and detection by electron-ionisation (EI) single quadrupole MS. Analysis was performed by an Agilent 6890 Series GC system with 7683 Autosampler/Injector unit, coupled to a 5973N Series quadrupole MS (Agilent Technologies; CA, USA). The injection temperature was set at 230ºC with a GC column initial temperature of 70ºC ramped at 1ºC/min for 5 min followed by 5.63ºC/min to 330ºC final temperature held for 10 min. The GC column was a 30 m Factor Four fused silica capillary column VF-5MS (ID = 0.25 mm, DF = 0.25 µm) with a 10 m EZ-Guard column (Agilent Technologies) and the carrier gas was helium set to a constant flow rate of 1 mL/min. The retention time was locked to elute a standard mannitol-TMS compound at 30.6 min. The transfer line into the MS was set at 280ºC and the ionisation source at 230ºC. Electron ionisation was set at -70 eV and the MS scan monitoring in mass range *m/z* 45-600 at a rate of 1.56 scans/sec.

Data processing and statistical analysis

Deconvolution of GC-MS data was performed using AnalyzerPro v5.2.1.6441 (SpectralWorks Ltd.; Runcorn, UK). Manual inspection and peak alignment of the resulting peak area matrix using the retention index (RI) ladder was carried out to reduce the occurrence of misallocated peaks and thus false positives. Identification of GC-MS peaks was achieved by comparing the mass spectra and RI with those of reference compounds from an in-house library of standards (Separation Science and Metabolomics Laboratory, and Metabolomics Australia; WA, Australia). In addition, a number of "unknown" metabolites were putatively annotated through comparison of the mass spectra with those of compounds in the commercially available NIST (National Institute of Standards and Technology; MD, USA) MS library. Only those features with >80% probability match factor to the NIST MS library were annotated as such. All other features were deemed as "Unknown" with respective retention time, RI, and base-peak spectral masses to distinguish them. For the peak area matrix, features which occurred in less than 80% of all samples were removed from subsequent analyses, unless their presence was unique to a particular treatment group in >75% of replicates. All remaining peak areas were normalised to the peak area of the internal standard compound to remove variation from any differences in extraction or instrumental procedures, and then normalised to the viable cell number in the parallel sample to remove variation from the different amounts of tissue analysed. The internal standard compound, and the *n*-alkane RI markers were then removed from the peak area matrix before statistical analyses, and the total number of detected features recorded.

The process of statistical analysis was repeated as described previously for untargeted metabolomics by GC-MS (Francki et al 2016), and a brief outline follows. For all multivariate and univariate statistical analyses, the peak areas (X) were first transformed using the equation $\log_{10}(X + 1)$. Principal component analysis (PCA) of both the permethrin-exposure and malathion-exposure peak area matrices (using a maximum 7 principal components, non-linear iterative partial least squares algorithm, no rotation, full cross validation, constant weighting and mean-centred data) was conducted using The Unscrambler X v10.3 (Camo; Oslo, Norway) and assessed for any spatial grouping and separation of different treatment groups which would indicate a change in the overall metabolite profile. Using PCA, those metabolites that most contributed to the spatial separation could be identified from the X-loadings plots that correspond to the PCA scores plots. For all univariate statistical analyses, the data were considered to be non-normally distributed with unequal variances for the most conservative calculation of significant differences between a relatively small number of replicates, and a two-tailed Student's t-test was used to determine the effects of acute exposure of permethrin or malathion on viable cell number and metabolite peak area. Statistically significant changes were considered for $P < 0.05$. Fold changes in the mean relative abundance of each metabolite feature between non-exposed and exposed groups were calculated using non-transformed, normalised peak areas. The metabolites with substantial (>2.0 or < 0.5) fold changes were grouped according to compound class (if identified) and the numbers of each recorded.

Results

B50 cells display distinct growth and metabolite profiles following exposure to permethrin or malathion

Immediately preceding sampling for metabolomic analysis, a parallel sample of each replicate was counted for viable cell number in order to correct the metabolite abundance data for any differences in the amount of tissue analysed. Figure 1 shows cell number and percentage viability as histograms to observe the gross effect of the insecticides on cell growth. The control groups ("No exposure") show that in normal growth conditions, the total cell number increased from 4.7×10^6 cells to 8.1×10^6 cells over 24 hours, an increase of 72%, which is an expected rate of growth for this cell line in ideal conditions (Otey et al 2003). Following exposure to permethrin or malathion the same growth rate was not observed. Interestingly, the cells exhibited a different response to each insecticide chemical. Permethrin exposure from 0 to 24 hours resulted in an 8.5% increase, while malathion exposure had a 29.8% decrease over the same time. Comparing the control to exposure groups at each time point, the number of viable cells at 6 hours was similar for all groups; only the permethrin-exposed group showed a significant 18.5% decrease from control ($P = 0.03846$), with no distinct difference in the malathion-exposed group. At 24 hours the effect of the chemical exposure on cell growth and survival became apparent, as both insecticides showed significant decrease in viable cells from control; permethrin exposure resulted in 37.0% fewer cells than control at the same time point ($P = 0.00021$), and malathion exposure caused a greater reduction, with 59.4% fewer cells ($P = 7.262 \times 10^{-6}$). The percentage of viable cells of total cell number remained the same across all groups at all time points, despite the observed reduction in cell number.

Photographs taken of all groups at 6 and 24 hours (Figure 2) are consistent with the cell number data, in that there was no marked visual difference in the cell culture of all groups at the 6-hour time point, yet at 24 hours there was an obvious difference in cell number in both exposure groups compared to the control group. For both exposure groups, there not only appears to have been a change in the number of cells present, but also an altered appearance of the cells themselves, indicating that the pesticide exposure has affected morphology. Both exposure groups appeared to have a more distorted, uneven outer membrane compared to unexposed cells, and malathion-exposed cells appeared to have less extended processes, and a slightly swollen cell body, compared to permethrin exposure and the control.

To characterise the overall impact of insecticide chemical exposure on the metabolite profile, we used a pattern recognition approach based on PCA of normalised peak areas for all observable features that had >80% coverage across all samples or a unique appearance within specific treatment groups, for both sets of insecticide-exposed cells (121 and 95 intracellular metabolites total, for permethrin- and malathion-exposed profiles, respectively). A full list of these metabolites, with fold-changes from control and P values, is included in supporting information (Tables S1 and S2). As this was an untargeted investigation, features with unknown identification were also included in analysis. There were 53 features of unknown identification, and 68 features of putative identification from either the in-house mass spectral library or a high-probability match with the NIST MS database, for the permethrin-exposure cell group. There were 34 unknowns, and 61 putatively identified features for the malathion-exposure cell group. Figure 3 shows the PCA plots of all time points of each insecticide exposure and their control groups, and revealed that all separate groups examined produced consistently altered metabolite profiles. Further PCA was conducted to investigate the difference between control and exposure groups at each time point, and the accompanying metabolite loadings plots for each were examined for those metabolites that contributed to the observed variation in metabolite profile (supporting information, Figure S1).

Analysis of PCA intracellular metabolite loadings identifies metabolites associated with exposure to an insecticide chemical

From the list of metabolite loadings, the fold change in relative abundance from control was calculated as well as the P value (Tables S1 and S2), and only those considered to be a major fold change (>2.0 or <0.5) in either the 6- or 24-hour time point were selected for further interpretation in this study (75 metabolites for permethrin exposure, and 72 for malathion exposure). Figure 4 shows these fold changes as histograms of metabolites in compound classes that showed a different trend between the two insecticide exposures, inclusive of amino acids, fatty acids, and intermediates of the TCA cycle (dicarboxylic acids and pyruvate). Histograms of the remaining metabolite classes that showed substantial fold changes are included in supporting information (Figure S2), for carbohydrates including monosaccharides and sugar alcohols, a small number of miscellaneous metabolites inclusive of lactate and uracil, and a large number of "unknowns".

Comparison of intracellular metabolite concentrations at different times of exposure were distinct for two separate classes of insecticide chemical

It was observed that there was a marked difference in metabolite response of B50 cells to the different insecticides permethrin and malathion, visualised by the fold change histograms in Figure 4. Permethrin-exposure resulted in seven amino acid features that had an altered abundance considered substantially different from control levels, whereas malathion-exposure resulted in 21 amino acid features whose abundance was substantially altered. The reverse trend was observed with fatty acids, where there were eight fatty acid metabolites that responded following permethrin exposure, and only two identified fatty acid metabolites that had a substantial fold change following malathion exposure. Overall, it can be observed that permethrin-exposure resulted in a predominantly fatty acid-based response, whereas malathion-exposure resulted in a predominantly amino-acid based response.

Perhaps the most marked difference in the direction of metabolite response between the two insecticide chemical exposures was in the TCA (tricarboxylic acid) cycle group (Figure 4); inclusive of dicarboxylic acid intermediates as well as pyruvate, all of which are important in energy synthesis for the cell. In particular, succinate and malate showed a significantly increased fold change after both 6 and 24 hours exposure to permethrin, while the opposite response occurred following malathion exposure with a significant decrease from control of the same two metabolites after 24 hours exposure. In both cases, changes in pyruvate were opposite to that of these metabolites. Pyruvate was substantially decreased following exposure to permethrin, where the TCA cycle intermediates were increased, while with malathion-exposure, pyruvate was substantially increased, where the TCA cycle intermediates were decreased.

The number of "unknown" metabolites for both insecticide exposures was similar. There was also a differing overall response of the "unknowns" for each metabolome (Figure S2, Supplementary Information), the overall trend for permethrin-exposure was a majority fold change increase from control after 24 hours of exposure, which was not seen to the same extent at 6 hours. For malathion-exposure, the overall trend was a majority fold change increase from

control after 6 hours of exposure, and for many of the same metabolites, this trend shifted to a decrease in fold change after 24 hours. Interestingly, there were a small number of "unknowns" that showed enormous increased in abundance following insecticide exposure, not matched by any of the identified metabolite features. These included a 28-fold increase in one metabolite ("Unknown_40.67_2585_91, 129…", Figure S2) after 24 hours of permethrin exposure, and four other features that had greater than 5-fold increase after either 6 and/or 24 hours ("Unknown_18.27_1334_189, 292", "Unknown_23.39_1551_117, 170", "Unknown_24.04_1584_147, 334" and "Unknown_24.58_1611_113, 198", Figure S2). Following malathion-exposure, there was one unknown feature ("Unknown_19.75_1394_147, 241, …", Figure S2) with a 33-fold increase after 6 hours, which was not maintained at 24 hours; the same feature was still present, but with only a 2.8-fold increase. There were two other features that exhibited a vast exaggerated abundance after 6 hours of malathion exposure, at 19- and 15-fold increases ("Unknown_18.06_1325_315, 330, 147" and "Unknown_27,44_1755_117, 363" respectively, Figure S2). The "unknowns" histograms display an overall difference between the two insecticide exposures; the majority of unknown features with a substantial fold change from control showed an increased response after 24 hours of permethrin exposure that was not seen to the same extent at 6 hours, indicating a progressive response or a 'build-up' of these particular metabolites in the B50 cells. An opposite overall trend was observed for malathion-exposure, where the larger, substantial fold changes occurred after 6 hours of exposure, and the response actually decreased from 6 to 24 hours, indicating a deterioration or conversion of these metabolites in B50 cells.

Discussion

This study has successfully observed differences in the intracellular metabolome profile of cultured neuronal B50 cells, and associated some of the specific differences to insecticide chemical exposure. From this untargeted metabolomic analysis of cultured cells, hundreds of individual metabolite features were able to be detected (Tables S1 and S2) and a great proportion (>50%) of those contributed to a change in the metabolome following a toxic insult (Figures 4 and S2). Principal component analysis of all samples showed that biological replicates grouped together and that specific metabolites could be distinguished for each time point of toxic exposure (Figures 3 and S1). This, together with the outcome of a large number of different classes of metabolites that were able to be detected, highlights the suitability of this cultured cell metabolomics model to monitor the cellular metabolic response to a toxic chemical exposure, and its potential for application to future toxicology testing practices. In the proposed 21st century model for toxicology testing and research (NRC 2007, Ramirez et al 2013), there are increasing demands for the use of human-derived cell lines coupled to molecular profiling platforms such as metabolomics, as a predictor for toxic adverse effects on key cellular pathways and metabolic events, not just in the advancement of current toxicology knowledge, but as an alternative to the use of animals in toxic chemical testing. One important future development would be the validation of the metabolic response in a human neuronal cell line, and the subsequent comparison to the rat B50 neuronal cell line.

Previous studies have investigated the metabolomic response in rats following exposure to different classes of pesticide chemicals, however only comparing the abundance of selected 'biomarker' molecules from the urine (Jones et al 2013, Liang et al 2013) and serum

metabolomes (Liang et al 2012, Moser et al 2015). The benefit of this cell culture metabolomics study in comparison to animal-based, 'biomarker' measurements is not only in the direct analysis of the intracellular metabolome of the cell type of interest, but also in the untargeted profiling of all detectable features that allow for the comparison of not just relative abundance, but also the quantity of substantially effected metabolites from particular classes, or of a particular pathway, that are altered from exposure to different toxic chemicals. Untargeted metabolomics is proposed to become the future direction of all metabolomics investigations (Sévin et al 2015) and is important for the interpretation of the biological response from metabolomics data, especially in relation to mechanistic toxicology studies and predicting potential harm from environmental chemicals (Aliferis and Chrysayi-Tokousbalides 2011).

This study was successful in determining that a distinct response is interpretable for different chemical exposures. Metabolic changes from exposure of rats to different pesticides has been recorded by previous studies (Liang et al 2012, Liang et al 2013, Moser et al 2015), although in some cases, such as permethrin exposure, the observed metabolic responses were not consistent. Liang et al (2013) reported an increase in free amino acids in the serum of rats following long-term (60 days) exposure to permethrin. A separate study comparing the response from multiple classes of pesticide chemicals found that there was no substantial change in amino acids in rats treated with a high dose of permethrin for 2 hours (Moser et al 2015). In this study, the response of amino acids to permethrin exposure was varied, with some increasing and others decreasing (Figure 4 and Table S1), indicating that there is some response to the pesticide exposure, but that it is not a one-way effect. The response of amino acids may be indicative of other energy metabolism processes (e.g. glycolysis or fatty acid β-oxidation) being the focus of toxic effect, and that altered usage or production of amino acids is an indirect effect. For example, this study observed that permethrin-exposure had a predominantly increased fatty acid-based response in the metabolome. Permethrin, a type I pyrethroid for which the neurotoxic action involves prolonging sodium channel activation resulting in depolarisation and neuronal excitotoxicity (Soderlund 2012), is known to induce an oxidative effect within cells that leads to lipid peroxidation (Abdollahi et al 2004, Banerjee et al 2001, Issam et al 2011).

In this study, exposure to malathion had a predominantly greater amino acid response than permethrin, evident from the number of substantial fold changes observed within the metabolite class (Figure 4) compared to that seen in permethrin exposure. Malathion, an organophosphate for which neurotoxic action is the inhibition of the enzyme acetylcholinesterase resulting in increased cholinergic signal transduction and excitotoxicity (Stenersen 2004), is known to elicit an excessive generation of reactive oxygen species (ROS) and cause a state of oxidative stress within cells (Ojha et al 2013). However, this study suggests that malathion toxicity may also manifest via glutamate excitotoxicity, evident from the 13-fold increase in pyroglutamate following 6 hours of malathion exposure (Figure 4). Pyroglutamate is the cyclised form of glutamate, and it is known that glutamate can be freely and non-enzymatically converted to pyroglutamate under high temperature conditions, such as within an ionisation source for analysis by MS (Purwaha et al 2014), and so levels of pyroglutamate can be considered indicative of changes in glutamate. Glutamate is the chief excitatory neurotransmitter in the mammalian nervous system and is known to be implicated in a wide variety of neurological pathologies (Choi 1988, Tian et al 2012, Veyrat-Durebex et al 2016, Ward et al 2000). Previous

investigations have shown that under stressed conditions neuronal cells will have an enhanced production of glutamate (Nishizawa 2001) and that, as a protective mechanism against glutamate-mediated excitotoxicity, cells may attempt to reduce the accumulation of glutamate by converting it into other amino acids (Wang and Qiu 2010). The overall, substantial increase in most detectable amino acid compounds observed in this study after 6 hours of malathion exposure supports an attempted protective mechanism against glutamate-mediated excitotoxicity in the response to malathion exposure. To provide mechanistic evidence for this speculation, future metabolomics studies could include cultured cells supplemented with radioisotope-labelled glutamine, as a way of tracking the directional flow through metabolic pathways of glutamine to glutamate, and the conversion into other amino acids (Mueller 2013, Sims 2013).

In this study the most notable, specific difference between the two insecticide exposures was that of the TCA cycle intermediates and pyruvate (Figure 4), where both chemical exposures resulted in substantial and opposite responses from control in these metabolites, indicating that energy synthesis was disrupted in both circumstances to different extents. Pyruvate had the opposite response to the TCA cycle intermediates with both permethrin and malathion exposure. Permethrin exposure showed decreased pyruvate abundance compared to increased TCA cycle intermediates, while malathion exposure showed an increased abundance of pyruvate compared to decreased TCA cycle intermediates. Further to the earlier suggestion of glutamate-mediated excitotoxicity in malathion-exposed cells, it may be possible that if glutamate was being converted into other amino acids as an attempted protective mechanism, this would reduce the glutamate available to power the TCA cycle (via the glutamate/glutamine cycle) (McKenna 2007, Peng et al 1993), and so account for the significantly decreased abundance of TCA cycle intermediates in malathion-exposed cells at 24 hours (Figure 4). A limitation to this is that an enzyme involved in the glutamate/glutamine cycle, glutamine synthetase, is specifically located in astrocytes, and not in neurons (Peng et al 1993), implying that this is not the mechanism occurring in our neuronal cell model. The same is true for an important TCA cycle enzyme, pyruvate carboxylase, also located specifically in astrocytes (Westergaard et al 1995). It is therefore likely that the observed effect on the TCA cycle was due to utilisation of the intermediate metabolites, as opposed to production. The switch from TCA cycle metabolism to predominantly glycolytic metabolism would drastically reduce available energy levels in the cell and have an impact on cell survival; which would account for the significant decrease in the number of viable cells after malathion exposure compared to no exposure at 24 hours (Figure 1, A). This was also an observed difference in response to permethrin exposure which had increased levels of TCA cycle intermediates compared to no exposure, and significantly more viable cells present than for malathion exposure at 24 hours.

Interestingly, previous studies on permethrin-exposure in rats showed the opposite results to this study and a decrease in TCA cycle intermediates (malate, citrate, and 2-oxoglutarate) following exposure to permethrin (Liang et al 2012, Liang et al 2013), yet they did not report on glycolytic intermediates, or pyruvate. This suggests that further efforts into the interpretation of the central energy metabolic pathways is a hugely important area to advance in metabolomics studies. For example, pyruvate is a key molecule that interconnects many metabolic pathways within a cell. Not only important in energy production, being the output of glycolysis and the precursor molecule of the TCA cycle, it can also be converted into carbohydrates, fatty acids and the amino acid, alanine. To be able to further interpret the exact

directions that pyruvate follows through the network of pathways within cells, future studies are necessary to explore the response of the metabolome at varying doses to look at scale of response, as well as several times of exposure and use of stable isotope-labelled carbon sources (^{13}C-glucose and ^{13}C-glutamine) to investigate metabolic flux (Mueller and Heinzle 2013, Sims et al 2013, Wegner et al 2015).

Analysis of the substantial fold changes from control in the relative abundance of all metabolite features detected uncovered a range of different metabolic responses that were unique to exposure to permethrin or malathion (Figure 4 and S2). A more detailed analysis of these particular metabolite groups in future investigations may provide a clearer picture of the specific biochemical events occurring in the cellular response from exposure to these toxins. One noticeable aspect from the metabolite relative abundance histograms as well as the supporting tables (Tables S1 and S2), is the large margin of error for many of the mean fold changes. These error margins would be improved in future studies by the use of a larger sample size per treatment group, and the use of quality-control, pooled samples in order to correct for the variation in large-scale data sets encountered during metabolomics analyses (Broadhurst and Kell 2006).

The "unknown", or unidentified detected features were included in all multivariate statistical analyses and their weighting to the overall metabolic profile of the cells was utilised. Some of these "unknowns" could be assumed to be artefactual to gas chromatography or the sample preparation processes, and inclusion of blank extraction samples in future analyses would help to clean up this list of unidentified features of potential interest. Despite this, there were substantial fold changes in relative abundance in some of the "unknown" metabolite features (Figure S2), the scale of which was not seen in any of the putatively identified features both biological and artefactual, and so their potential as compounds of interest was noted. Due to the large error margins with these higher fold-change features, it is difficult to interpret any such changes, but they help to demonstrate that this metabolomics perspective can detect both high and low relative abundances of a diverse range of different metabolite classes, as a single snap-shot of toxic exposure metabolic response of a cell system. Future investigations should take into consideration the potential for margins of error with single-platform, low sample number studies, and take appropriate action to best fit the experimental design to the variety of data able to be collected.

In this study, the metabolic response was also compared to the observed numbers of viable cells and the appearance of cells in culture (Figures 1 and 2 respectively). Despite a reduction in cell number resulting from exposure to either insecticide, there was a distinct lack of reduction in cell viability (Figure 1). It can be assumed from this that the cell membranes remained intact until immediately before cell death. In the case for future cell culture metabolomics investigations, this cell type appears to be an optimal model for the detection of intracellular metabolites. The analysis of extracellular metabolites from this model may provide a clearer picture of the state of degraded cells that have released their internal metabolites into the surrounding medium. This could further uncover a living cell's metabolic state (Aurich et al 2015, Nicolae et al 2014) in the moments immediately preceding cell death, and comparison of this to intracellular metabolites of remaining viable cells may help to interpret where the 'points of no return' might be for the metabolic state of a cell in response to toxins.

Conclusions

Metabolomics has been proposed as a new and exciting technique to study the toxic effect of environmental chemicals and to test for their safety in mammalian cells. To investigate whether metabolomics can be used to elucidate the metabolic response of the mammalian nervous system to neurotoxic insecticide chemicals, we analysed the metabolome of cultured B50 neuroblastoma cells following exposure to the pyrethroid insecticide permethrin or the organophosphate insecticide malathion. Distinct effects on cell growth and the metabolite profile were observed for both toxic chemicals. This study has illustrated the ability of metabolomics to detect not only an overall change in the metabolome, but to further identify specific metabolic deviations which are particularly important for deducing the possible downstream effects on function and stability of the cell, heavily influenced by exposure to a potentially toxic chemical. In this new approach to examination of chemical toxicology, two differing classes of insecticide chemicals, permethrin and malathion, were both found to induce anti-oxidative stress defences, glutamate-mediated excitotoxicity, and disturbances in the TCA cycle in cultured neuronal cells.

This study provides proof of concept for future cultured cell metabolomics studies investigating the neurotoxic cellular response to environmental chemicals that may be adversely affecting human health. In order to further elucidate the finer details of the metabolic processes involved and the potential mechanisms behind development of disease, this study design should be expanded with multiple doses and varying time points of exposure which would give a greater understanding of the directional expression of the observed metabolite changes. With the expansion of this metabolomics knowledge of the cellular response to toxins, it may be possible to isolate specific responses to particular toxins, and the downstream effects that can result from chemical exposure, that have currently gone unnoticed and undefined. With more understanding of how chemical exposure has an effect on the metabolism of neuronal cells, it may be possible to define a pathway of disease development demonstrating how environmental chemicals may be implicated in the increasing prevalence of neurological disorders world-wide.

Acknowledgments

This work was supported in part by the National Collaborative Research Infrastructure Strategy Bioplatforms Australia, the Australian Government Research Training Program Scholarship, and the McCusker Charitable Foundation.

Disclosure

The authors declare that there are no competing financial or other conflicts of interest.

References

Abbiss H, Maker GL, Gummer J, Sharman MJ, Phillips JK, Boyce M, Trengove RD. 2012. Development of a non-targeted metabolomics method to investigate urine in a rat model of polycystic kidney disease. *Nephrology*. **17**:104-110. DOI: 10.1111/j.1440-1797.2011.01532.x

Abbiss H, Rawlinson C, Maker GL, Trengove R. 2015. Assessment of automated trimethylsilyl derivatization protocols for GC-MS-based untargeted metabolomic analysis of urine. *Metabolomics*. **11**:1908-1921. DOI: 10.1007/s11306-015-0839-y

Abdollahi M, Ranjbar A, Shadnia S, Nikfar S, Rezaie A. 2004. Pesticides and oxidative stress: a review. *Med Sci Monit*. **10**:141-147. URL: http://www.MedSciMonit.com/pub/vol_10/no_6/4163.pdf

Aliferis KA, Chrysayi-Tokousbalides M. 2011. Metabolomics in pesticide research and development: review and future perspectives. *Metabolomics*. **7**:35-53. DOI: 10.1007/s11306-010-0231-x

Ascherio A, Chen H, Weisskopf MG, O'Reilly E, McCullough ML, Calle EE, Schwarzchild MA, Thun MJ. 2006. Pesticide exposure and risk for Parkinson's Disease. *Ann Neurol*. **60**:197-203. DOI: 10.1002/ana.20904

Aurich MK, Paglia G, Rolfsson Ó, Hrafnsdóttir S, Magnúsdóttir M, Stefaniak MM, Palsson BØ, Fleming RMT, Thiele I. 2015. Prediction of intracellular metabolic states from extracellular metabolomic data. *Metabolomics*. **11**:603-619. DOI: 10.1007/s11306-014-0721-3

Babina K, Dollard M, Pilotto L, Edwards JW. 2012. Environmental exposure to organophosphorus and pyrethroid pesticides in South Australian preschool children: A cross sectional study. *Environ Int*. **48**:109-120. DOI: 10.1016/j.envint.2012.07.007

Banerjee BD, Seth V, Ahmed RS. 2001. Pesticide-induced oxidative stress: perspectives and trends. *Rev Environ Health*. **16**:1-40. DOI: 10.1515/reveh.2001.16.1.1

Becker K, Seiwert M, Angerer J, Kolossa-Gehring M, Hoppe H-W, Ball M, Schulz C, Thumulla J, Seifert B. 2006. GerES IV Pilot Study: Assessment of the exposure of German children to organophosphorus and pyrethroid pesticides. *Int J Hyg Environ Health*. **209**:221-233. DOI: 10.1016/j.ijheh.2005.12.002

Bouchard MF, Bellinger DC, Wright RO, Weisskopf MG. 2010. Attention-Deficit/Hyperactivity Disorder and urinary metabolites of organophosphate residues. *Pediatrics*. **125**:1270-1277. DOI: 10.1542/peds.2009-3058

Bouhifd M, Hartung T, Hogberg HT, Kleensang A, Zhao L. 2013. Toxicometabolomics. *J Appl Toxicol*. **33**:1365-1383. DOI: 10.1002/jat.2874

Broadhurst DI, Kell DB. 2006. Statistical strategies for avoiding false discoveries in metabolomics and related experiments. *Metabolomics*. **2**:171-196. DOI: 10.1007/s11306-006-0037-z

Choi DW. 1988. Glutamate neurotoxicity and diseases of the nervous system. *Neuron*. **1**:623-634. DOI: 10.1016/0896-6273(88)90162-6

Curtis CF, Mnzava AE. 2000. Comparison of house spraying and insecticide-treated nets for malaria control. *Bull World Health Organ*. **78**:1389-1400. DOI: 10.1590/S0042-96862000001200006

Egan H. 1966. Pesticide residues in fat-containing food and in human fat. *Proc Nutr Soc*. **25**:44-51. DOI: 10.1079/PNS19660010

Ellis JK, Athersuch TJ, Cavill R, Radford R, Slattery C, Jennings P, McMorrow T, Ryan MP, Ebbels TMD, Keun HC. 2011. Metabolic response to low-level toxicant exposure in a novel renal tubule epithelial cell system. *Mol Biosyst*. **7**:247-257. DOI: 10.1039/c0mb00146e

Fenske RA, Lu C, Barr D, Needham L. 2002. Children's exposure to chlorpyrifos and parathion in an agricultural communitiy in central Washington state. *Environ Health Perspect*. **110**:549-553. DOI: 10.1289/ehp.02110549

Flaskos J. 2012. The developmental neurotoxicity of organophosphorus insecticides: A direct role for the oxon metabolites. *Toxicol Lett*. **209**:86-93. DOI: 10.1016/j.toxlet.2011.11.026

Fragar LJ, Sankaran B, Thomas P. 2005. *Pesticides and Adverse Health Outcomes in Australia*. Rural Industries Research and Development Corporation: Barton, ACT.

Francki MG, Hayton S, Gummer JPA, Rawlinson C, Trengove RD. 2016. Metabolomic profiling and genomic analysis of wheat aneuploid lines to identify genes controlling biochemical pathways in mature grain. *Plant Biotechnol J*. **14**:649-660. DOI: 10.1111/pbi.12410

Hemingway J. 2014. The role of vector control in stopping the transmission of malaria: threats and opportunities. *Philos Trans R Soc Lond B Biol Sci*. **369**:20130431. DOI: 10.1098/rstb.2013.0431

Heudorf U, Angerer J, Drexler H. 2004. Current internal exposure to pesticides in children and adolescents in Germany: Urinary levels of metabolites of pyrethroid and organophosphorus insecticides. *Int Arch of Occup Environ Health*. **77**:67-72. DOI: 10.1007/s00420-003-0470-5

Huang S-M, Zuo X, Li JJE, Li SFY, Bay BH, Ong CN. 2012. Metabolomics studies show dose-dependent toxicity induced by SiO_2 nanoparticles in MRC-5 human fetal lung fibroblasts. *Adv Healthc Mater*. **1**:779-784. DOI: 10.1002/adhm.201200114

Issam C, Zohra H, Monia Z, Hassan BC. 2011. Effects of dermal subchronic exposure of pubescent rats to permethrin (PRMT) on the histological structures of genital tract, testosterone and lipoperoxidation. *Exp Toxicol Pathol*. **63**:393-400. DOI: 10.1016/j.etp.2010.02.016

Johnson CH, Patterson AD, Idle JR, Gonzalez FJ. 2012. Xenobiotic Metabolomics: Major impact on the metabolome. *Annu Rev Pharmacol Toxicol*. **52**:37-56. DOI: 10.1146/annurev-pharmtox-010611-134748

Jones OAH, Murfitt S, Svendsen C, Turk A, Turk H, Spurgeon DJ, Walker LA, Shore RF, Long SM, Griffin JL. 2013. Comparisons of metabolic and physiological changes in rats following short term oral dosing with pesticides commonly found in food. *Food Chem Toxicol*. **59**:438-445. DOI: 10.1016/j.fct.2013.06.041

Keifer MC, Firestone J. 2007. Neurotoxicity of pesticides. *J Agromedicine*. **12**:17-25. DOI: 10.1300/J096v12n01_03

Kohlmeier L, Kohlmeier M. 1995. Adipose tissue as a medium for epidemiologic exposure assessment. *Environ Health Perspect*. **103**:99-106. DOI: 10.1289/ehp.95103s399

Lee I, Eriksson P, Fredriksson A, Buratovic S, Viberg H. 2015. Developmental neurotoxic effects of two pesticides: Behavior and neuroprotein studies on endosulfan and cypermethrin. *Toxicology*. **335**:1-10. DOI: 10.1016/j.tox.2015.06.010

Liang YJ, Wang HP, Long DX, Wu YJ. 2012. Applying biofluid metabonomic techniques to analyze the combined subchronic toxicity of propoxur and permethrin in rats. *Bioanalysis*. **4**:2897-2907. DOI: 10.4155/bio.12.277

Liang YJ, Wang HP, Long DX, Li W, Wu YJ. 2013. A metabonomic investigation of the effects of 60 days exposure of rats to two types of pyrethroid insecticides. *Chem Biol Interact*. **206**:302-308. DOI: 10.1016/j.cbi.2013.10.002

Liu J, Schelar E. 2012. Pesticide exposure and child neurodevelopment: summary and implications. *Workplace Health Saf*. **60**:235-242. DOI: 10.3928/21650799-20120426-73

Lu C, Barr DB, Pearson MA, Walker LA, Bravo R. 2009. The attribution of urban and suburban children's exposure to synthetic pyrethroid insecticides: a longitudinal assessment. *J Expo Sci Environ Epidemiol*. **19**:69-78. DOI: 10.1038/jes.2008.49

Maroni M, Colosio C, Ferioli A, Fait A. 2000. Biological Monitoring of Pesticide Exposure: a review. Introduction. *Toxicology*. **143**:1-118

Marrs TC. 2012. Toxicology of insecticides to mammals. *Pest Manag Sci*. **68**:1332-1336. DOI: 10.1002/ps.3362

McKenna MC. 2007. The glutamate-glutamine cycle is not stoichiometric: fates of glutamate in brain. *J Neurosci Res*. **85**:3347-3358. DOI: 10.1002/jnr.21444

Mediani A, Abas F, Khatib A, Tan CP, Ismail IS, Shaari K, Ismail A, Lajis NH. 2015. Relationship between metabolites composition and biological activities of Phyllanthus niruri extracts prepared by different drying methods and solvents extraction. *Plant Foods Hum Nutr*. **70**:184-192. DOI: 10.1007/s11130-015-0478-5

Moretto A, Colosio C. 2011. Biochemical and toxicological evidence of neurological effects of pesticides: the example of Parkinson's disease. *Neurotoxicology*. **32**:383-391. DOI: 10.1016/j.neuro.2011.03.004

Moser VC, Stewart N, Freeborn DL, Crooks J, MacMillan DK, Hedge JM, Wood CE, McMahen RL, Strynar MJ, Herr DW. 2015. Assessment of serum biomarkers in rats after exposure to pesticides of different chemical classes. *Toxicol Applied Pharmacol*. **282**:161-174. DOI: 10.1016/j.taap.2014.11.016

Mueller D, Heinzle E. 2013. Stable isotope-assisted metabolomics to detect metabolic flux changes in mammalian cell cultures. *Curr Opin Biotechnol*. **24**:54-59. DOI: 10.1016/j.copbio.2012.10.015

Naeher LP, Tulve NS, Egeghy PP, Barr DB, Adetona O, Fortmann RC, Needham LL, Boseman E, Hilliard A, Sheldon LS. 2010. Organophosphorus and pyrethroid insecticide urinary metabolite concentrations in young children living in a southeastern United States city. *Sci Total Environ*. **408**:1145-1153. DOI: 10.1016/j.scitotenv.2009.10.022

Narahashi T. 2010. Neurophysiological effects of insecticides. In *Hayes' Handbook of Pesticide Toxicology*, Vol. 1, Krieger R (ed). Academic Press: London, UK; 799-817

Ng JS, Ryan U, Trengove RD, Maker GL. 2012. Development of an untargeted metabolomics method for the analysis of human faecal samples using Cryptosporidium-infected samples. *Mol Biochem Parasitol*. **185**:145-150. DOI: 10.1016/j.molbiopara.2012.08.006

Nicolae A, Wahrheit J, Bahnemann J, Zeng A-P, Heinzle E. 2014. Non-stationary ^{13}C metabolic flux analysis of Chinese hamster ovary cells in batch culture using extracellular labeling highlights metabolic reversibility and compartmentation. *BMC Syst Biol*. **8**:50-64. DOI: 10.1186/1752-0509-8-50

Nishizawa Y. 2001. Glutamate release and neuronal damage in ischemia. *Life Sci*. **69**:369-381. DOI: 10.1016/S0024-3205(01)01142-0

National Research Council (NRC). 2007. *Toxicity Testing in the 21st Century: A Vision and a Strategy*. Washington DC, USA:National Research Council (NRC).

Ojha A, Yaduvanshi SK, Pant SC, Lomash V, Srivastava N. 2013. Evaluation of DNA damage and cytotoxicity induced by three commonly used organophosphate pesticides individually and in mixture, in rat tissues. *Environ Toxicol*. **28**:543-552. DOI: 10.1002/tox.20748

Otey CA, Boukhelifa M, Maness P. 2003. B35 neuroblastoma cells: an easily transfected, cultured cell model of central nervous system neurons. *Methods Cell Biol*. **71**:287-304. DOI: 10.1016/S0091-679X(03)01013-6

Peng L, Hertz L, Huang R, Sonnewald U, Petersen SB, Westergaard N, Larsson O, Schousboe A. 1993. Utilization of glutamine and of TCA cycle constituents as precursors for transmitter glutamate and GABA. *Dev Neurosci*. **15**:367-377. DOI: 10.1159/000111357

Purwaha P, Silva LP, Hawke DH, Weinstein JN, Lorenzi PL. 2014. An artifact in LC-MS/MS measurement of glutamine and glutamic acid: In-source cyclization to pyroglutamic acid. *Anal Chem*. **86**:5633-5637. DOI: 10.1021/ac501451v

Qin XY, Akanuma H, Wei F, Nagano R, Zeng Q, Imanishi S, Ohsako S, Yoshinaga J, Yonemoto J, Tanokura M, Sone H. 2012. Effect of low-dose thalidomide on dopaminergic neuronal differentiation of human neural progenitor cells: A combined study of metabolomics and morphological analysis. *Neurotoxicology*. **33**:1375-1380. DOI: 10.1016/j.neuro.2012.08.016

Ramirez T, Daneshian M, Kamp H, Bois FY, Clench MR, Coen M, Donley B, Fischer SM, Ekman DR, Fabian E, Guillou C, Heuer J, Hogberg HT, Jungnickel H, Keun HC, Krennrich G, Krupp E, Luch A, Noor F, Peter E, Riefke B, Seymour M, Skinner N, Smirnova L, Verheij E, Wagner S, Hartung T, van-Ravenzwaay B, Leist M. 2013. Metabolomics in toxicology and preclinical research. *ALTEX*. **30**:209-225. DOI: 10.14573/altex.2013.2.209

Roberts EM, English PB, Grether JK, Windham GC, Somberg L, Wolf C. 2007. Maternal residence near agricultural pesticide applicaitons and autism spectrum disorders among children in the California central valley. *Envron Health Perspect*. **115**:1482-1489. DOI: 10.1289/ehp.10168

Searles Nielson S, McKean-Cowdin R, Farin FM, Holly EA, Preston-Martin S, Mueller BA. 2010. Childhood brain tumors, residential insecticidal exposure, and pesticide metabolism genes. *Environ Health Perspect*. **118**:144-149. DOI: 10.1289/ehp.0901226

Sévin DC, Kuehne A, Zamboni N, Sauer U. 2015. Biological insights through nontargeted metabolomics. *Curr Opin Biotechnol*. **34**:1-8. DOI: 10.1016/j.copbio.2014.10.001

Sims JK, Manteiger S, Lee K. 2013. Towards high resolution analysis of metabolic flux in cells and tissues. *Curr Opin Biotechnol*. **24**:933-939. DOI: 10.1016/j.copbio.2013.07.001

Snouber LC, Bunescu A, Naudot M, Legallais C, Brochot C, Dumas ME, Elena-Herrmann B, Leclerc E. 2013. Metabolomics-on-a-chip of hepatotoxicity induced by anticancer drug flutamide and its active metabolite hydroxyflutamide using HepG2/C3a microfluidic biochips. *Toxicol Sci*. **132**:8-20. DOI: 10.1093/toxsci/kfs230

Soderlund DM. 2012. Molecular mechanisms of pyrethroid insecticide neurotoxicity: Recent advances. *Arch Toxicol*. **86**:165-181. DOI: 10.1007/s00204-011-0726-x

Stenersen J. 2004. *Chemical Pesticides: Mode of Action and Toxicology*. CRC Press: Florida, USA.

Tian C, Sun L, Jia B, Ma K, Curthoys N, Ding J, Zheng J. 2012. Mitochondrial glutaminase release contributes to glutamate-mediated neurotoxicity during human immunodeficiency virus-1 infection. *J Neuroimmune Pharmacol*. **7**:619-628. DOI: 10.1007/s11481-012-9364-1

Timofeeva OA, Levin ED. 2010. Lasting behavioural consequences of organophosphate pesticide exposure during development. In *Hayes' Handbook of Pesticide Toxicology*, Vol. 1, Krieger R (ed). Academic Press: London, UK.; 837-846

Van den Hof WFPM, Ruiz-Aracama A, Van Summeren A, Jennen DGJ, Gaj S, Coonen MLJ, Brauers K, Wodzig WKWH, van Delft JHM, Kleinjans JCS. 2015. Integrating multiple omics to unravel mechanisms of Cyclosporin A induced hepatotoxicity *in vitro*. *Toxicol In Vitro*. **29**:489-501. DOI: 10.1016/j.tiv.2014.12.016

van Vliet E, Morath S, Eskes C, Linge J, Rappsilber J, Honegger P, Hartung T, Coecke S. 2008. A novel *in vitro* metabolomics approach for neurotoxicity testing, proof of principle for methyl mercury chloride and caffeine. *Neurotoxicology*. **29**:1-12. DOI: 10.1016/j.neuro.2007.09.007

Veyrat-Durebex C, Corcia P, Piver E, Devos D, Dangoumau A, Gouel F, Vourc'h P, Emond P, Laumonnier F, Nadal-Desbarats L, Gordon PH, Andres CR, Blasco H. 2016. Disruption of TCA cycle and glutamate metabolism identified by metabolomics in an *in vitro* model of amyotrophic lateral sclerosis. *Mol Neurobiol*. **53**:6910-6924. DOI: 10.1007/s12035-015-9567-6

Wang Y, Qiu ZH. 2010. Molecular and cellular mechanisms of excitotoxic neuronal death. *Apoptosis*. **15**:1382-1402. DOI: 10.1007/s10495-010-0481-0

Ward MW, Rego AC, Frenguelli BG, Nicholls DG. 2000. Mitochondrial membrane potential and glutamate excitotoxicity in cultured cerebellar granule cells. *J Neurosci*. **20**:7208-7219. DOI: 10.1.1.336.7775

Wegner A, Meiser J, Weindl D, Hiller K. 2015. How metabolites modulate metabolic flux. *Curr Opin Biotechnol*. **34**:16-22. DOI: 10.1016/j.copbio.2014.11.008

Welsh-Bohmer KA, Plassman BL, Hayden KM. 2010. Genetic and envrionmental contributions to cognitive decline in aging and Alzheimer's disease. *Annu Review Gerontol Geriatr*. **30**:81-114. DOI: 10.1891/0198-8794.30.81

Wenner MI, Maker GL, Dawson LF, Drummond PD, Mullaney I. 2016. The potential of metabolomic analysis techniques for the characterisation of α1-adrenergic receptors in cultured N1E-115 mouse neuroblastoma cells. *Cytotechnol*. **68**:1561-1575. DOI: 10.1007/s10616-015-9915-4

Westergaard N, Sonnewald U, Schousboe A. 1995. Metabolic trafficking between neurons and astrocytes: the glutamate/glutamine cycle revisited. *Dev Neurosci*. **17**:203-211. DOI: 10.1159/000111288

Zaganas I, Kapetanaki S, Mastorodemos V, Kanavouras K, Colosio C, Wilks MF, Tsatsakis AM. 2013. Linking pesticide exposure and dementia: what is the evidence? *Toxicology*. **307**:3-11. DOI: 10.1016/j.tox.2013.02.002

Zurich MG, Monnet-Tschudi F. 2009. Contribution of *in vitro* neurotoxicology studies to the elucidation of neurodegenerative processes. *Brain Res Bull*. **80**:211-216. DOI: 10.1016/j.brainresbull.2009.06.008

Figure Legends

Figure 1

B50 cells following acute exposure to permethrin or malathion for 6 and 24 hours, counted using the Trypan blue exclusion method. A: Mean total number of viable cells ($x10^6$), and B: mean percentage cell viability. Control cells ('No exposure') were counted at 0 hours (time of treatment) as well as at both 6 and 24 hours and combined to obtain the overall mean. n=8 for "No exposure" group, n=4 for "+ Permethrin" and "+ Malathion" groups. Error bars indicate 1 x standard error from the mean. Significant difference in cell number to the control is shown by * where $P < 0.05$ and *** where $P < 0.0005$. There were no observed significant differences in the percentage cell viability.

Figure 2

B50 cells photographed under inverted light microscope magnification. Images are of cell samples set up for metabolite profiling analysis and show cells following both 6 and 24 hours of A: no exposure (control), B: acute exposure to permethrin (200 µg/mL), and C: acute exposure to malathion (200 µg/mL). Note: due to the lowered solubility of permethrin in aqueous solution, the insolubilised portion of the insecticide formulation can be seen in the images in row B, as small particulates present in the medium.

Figure 3

PCA scores plots showing the response of B50 cells to acute exposure of A: permethrin or B: malathion for 6 and 24 hours. PCA was applied to the intracellular metabolite profiles to assess effects of insecticide exposure. Plots show both control (No exposure) and insecticide-exposed cells for both time points. In plot A, n=4 for all treatment groups. In plot B, n=4 for "No exposure 24 hours" and "+ Malathion 6 hours" groups, and n=3 for "No exposure 6 hours" and "+ Malathion 24 hours", due to the removal of outlier samples. Each PCA plot was further analysed (see supporting information, Figure S1) by separate PCA on samples from each time of exposure only, and the associated loadings plots used to investigate the metabolites that corresponded to a change in profile between control and treatment groups.

Figure 4

Fold change histograms showing the effect of insecticide chemical exposure on the relative abundance of intracellular metabolites that had a substantial fold change from control (> 2.0 or < 0.5) in the B50 cell line. Histograms show metabolites from the compound classes amino acids, fatty acids, and dicarboxylic acids and pyruvate (TCA cycle), that were measured in the metabolome after either permethrin or malathion exposure and compares fold change in abundance after 6 and 24 hours of exposure. Error bars indicate 1 x standard error from the mean. Significantly different metabolite abundances in exposed cells relative to control is shown by * $P < 0.05$, ** $P < 0.005$, and *** $P < 0.0005$. TMS = Trimethylsilyl.

Figures

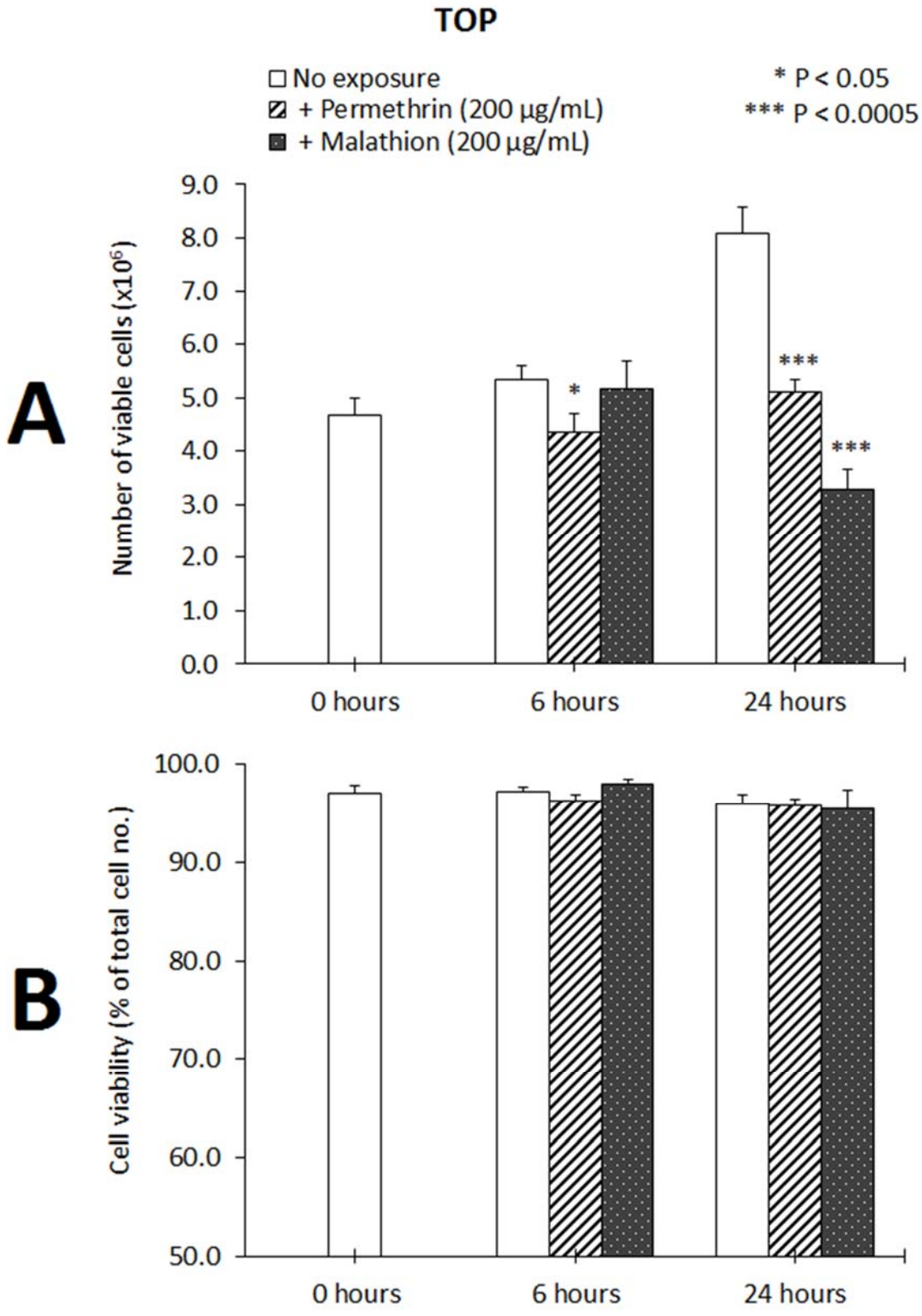

Figure 1

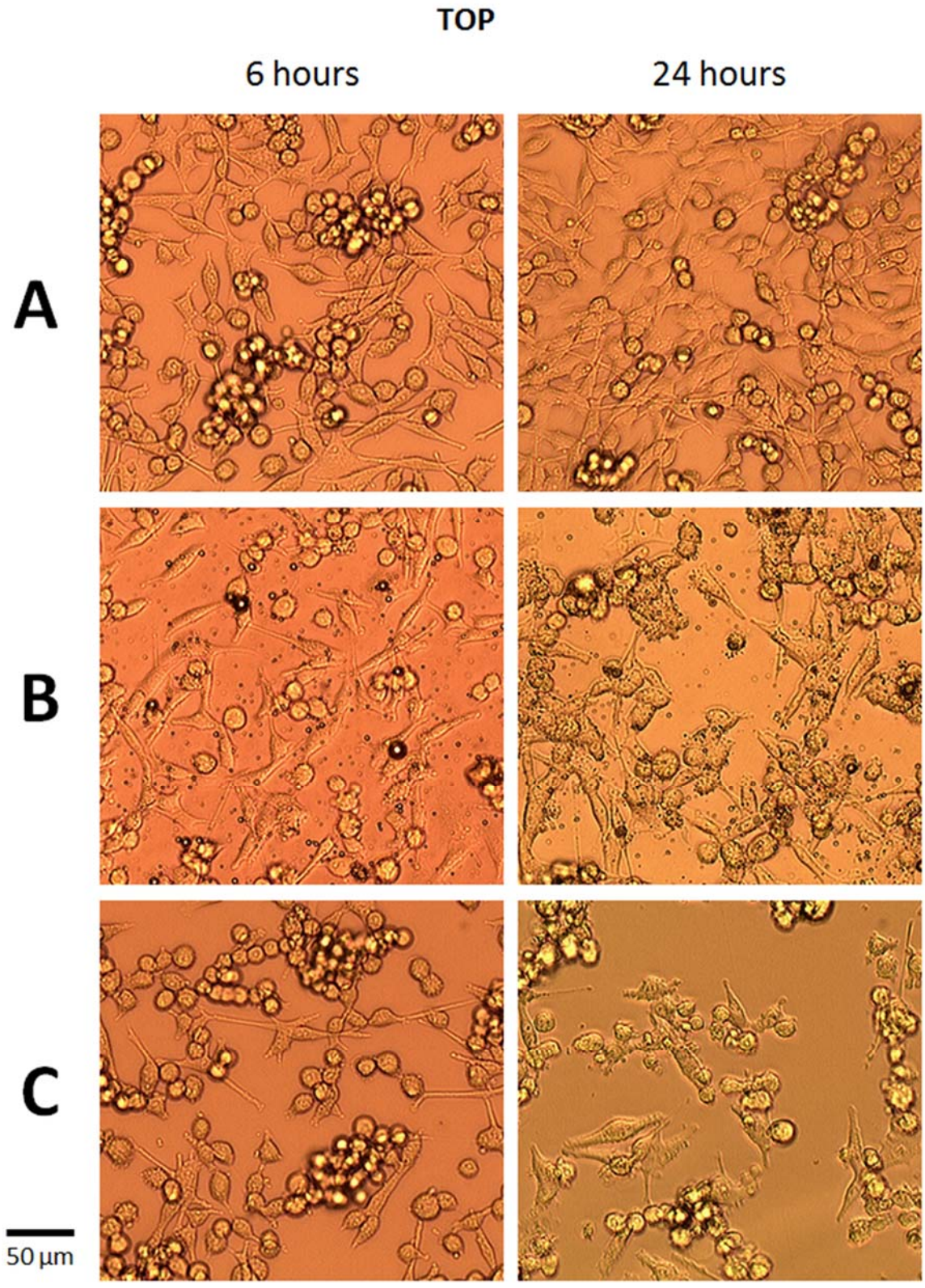

Figure 2

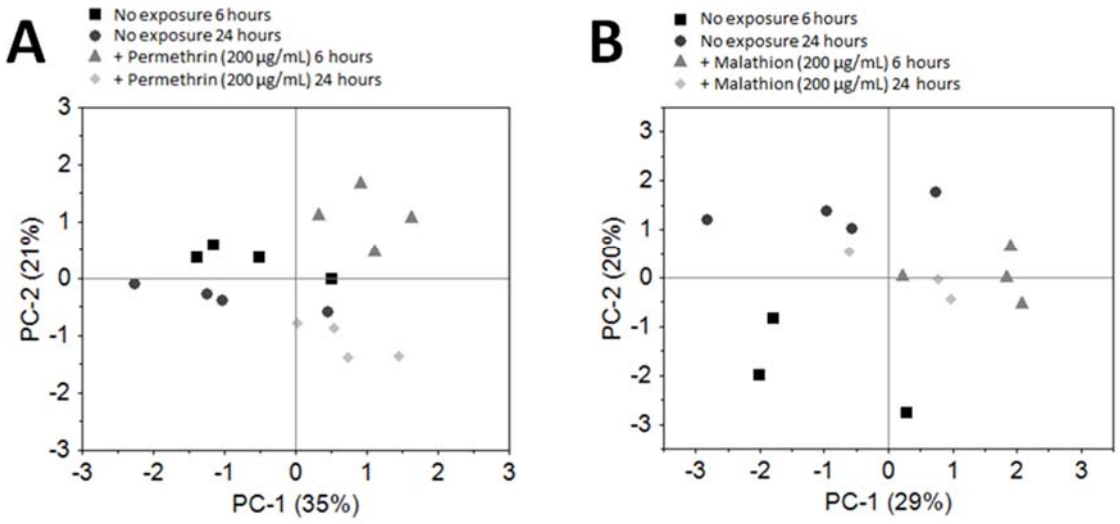
A
No exposure 6 hours
No exposure 24 hours
+ Permethrin (200 µg/mL) 6 hours
+ Permethrin (200 µg/mL) 24 hours
PC-2 (21%)
PC-1 (35%)
B
No exposure 6 hours
No exposure 24 hours
+ Malathion (200 µg/mL) 6 hours
+ Malathion (200 µg/mL) 24 hours
PC-2 (20%)
PC-1 (29%)

Figure 3

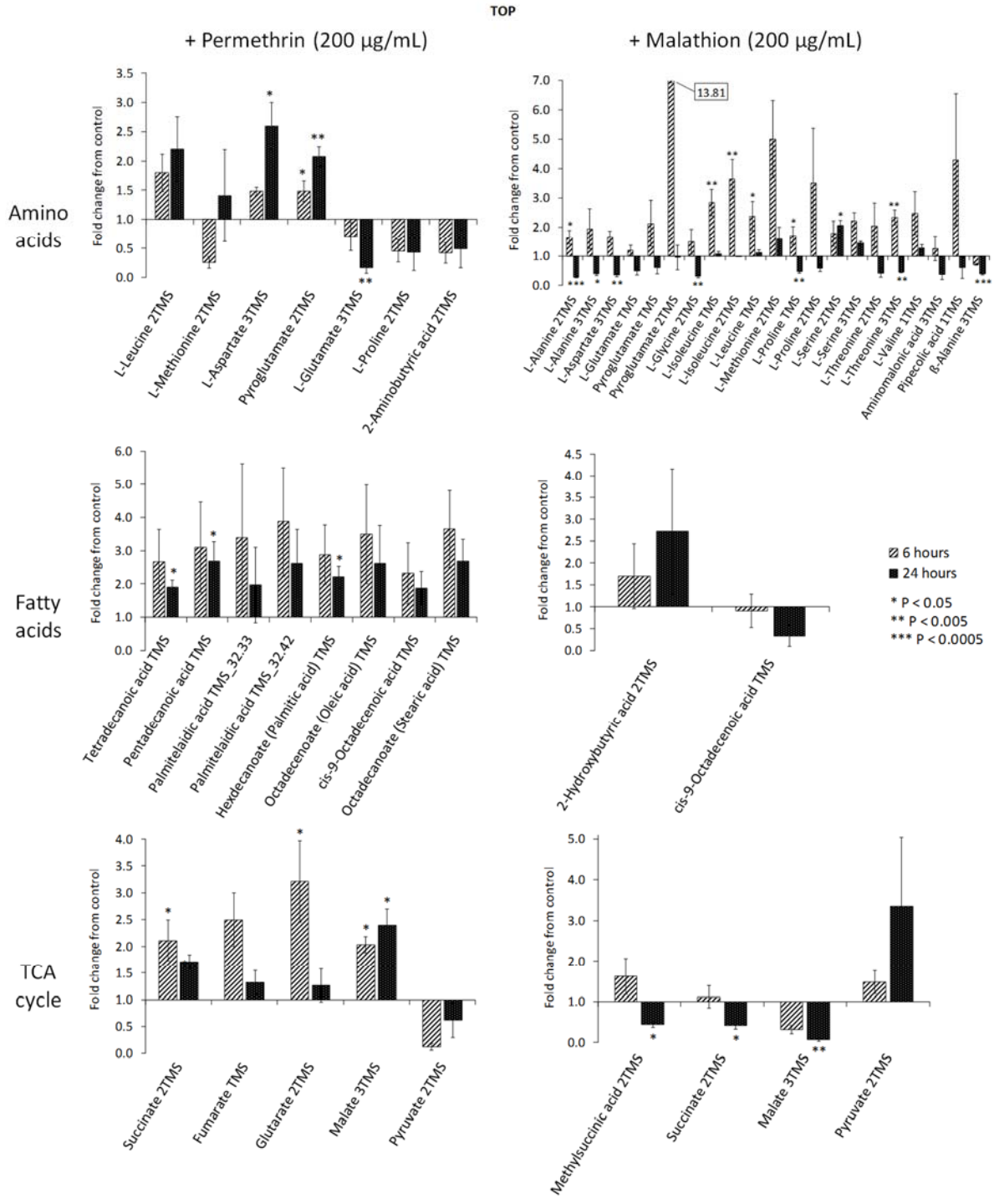
TOP
+ Permethrin (200 µg/mL)
+ Malathion (200 µg/mL)
Amino acids
Fatty acids
TCA cycle
Fold change from control
13.81
L-Leucine 2TMS
L-Methionine 2TMS
L-Aspartate 3TMS
Pyroglutamate 2TMS
L-Glutamate 3TMS
L-Proline 2TMS
2-Aminobutyric acid 2TMS
L-Alanine 2TMS
L-Alanine 3TMS
L-Aspartate 3TMS
L-Glutamate TMS
Pyroglutamate TMS
Pyroglutamate 2TMS
L-Glycine 2TMS
L-Isoleucine TMS
L-Isoleucine 2TMS
L-Leucine TMS
L-Methionine 2TMS
L-Proline TMS
L-Proline 2TMS
L-Serine 2TMS
L-Serine 3TMS
L-Threonine 2TMS
L-Threonine 3TMS
L-Valine 1TMS
Aminomalonic acid 3TMS
Pipecolic acid 1TMS
β-Alanine 3TMS
Tetradecanoic acid TMS
Pentadecanoic acid TMS
Palmitelaidic acid TMS_32.33
Palmitelaidic acid TMS_32.42
Hexadecanoate (Palmitic acid) TMS
Octadecenoate (Oleic acid) TMS
cis-9-Octadecenoic acid TMS
Octadecanoate (Stearic acid) TMS
2-Hydroxybutyric acid 2TMS
cis-9-Octadecenoic acid TMS
6 hours
24 hours
* P < 0.05
** P < 0.005
*** P < 0.0005
Succinate 2TMS
Fumarate TMS
Glutarate 2TMS
Malate 3TMS
Pyruvate 2TMS
Methylsuccinic acid 2TMS
Succinate 2TMS
Malate 3TMS
Pyruvate 2TMS

Figure 4

Supporting Information

Figure S1

PCA scores plots showing the response of B50 cells to acute exposure of permethrin or malathion for 6 and 24 hours. PCA was applied to the intracellular metabolite profiles to assess effects of insecticide exposure at separate times. The accompanying metabolite loadings plots were used to identify the metabolites that most contributed to the different profiles observed in PCA plots A: permethrin exposure for 6 hours, B: permethrin exposure for 24 hours, C: malathion exposure for 6 hours, and D: malathion exposure for 24 hours.

Figure S2

Fold change histograms showing the effect of insecticide chemical exposure on the relative abundance of intracellular metabolites that had a substantial fold change from control (> 2.0 or < 0.5) in the B50 cell line. Histograms show metabolites from the compound classes carbohydrates, miscellaneous "others", as well as the unknowns (unidentified features), that were measured in the metabolome after either permethrin or malathion exposure and compares fold change in abundance after 6 and 24 hours of exposure. Error bars indicate 1 x standard error from the mean. Significantly different metabolite abundances in exposed cells relative to control is shown by * $P < 0.05$, ** $P < 0.005$, and *** $P < 0.0005$.

Table S1

Intracellular metabolites of B50 cells following acute exposure to 200 mg/mL of the pyrethroid insecticide, permethrin for 6 and 24 hours. Metabolite compounds are listed by their chemical class. Fold changes in relative abundance from control and the associated P values are given for both 6 hour and 24 hour exposure times. Compound information includes but is not limited to retention time (RT (min)), retention index (RI), relative standard deviation of the average RI (RI RSD (%)), base peak mass/es (BP *m/z* (EI)) and compound identification parameters. Each compound is given an ID score based on a scale of identification criteria as proposed by Abbiss et al (2015). Table headings are defined as below the table.

Table S2

Intracellular metabolites of B50 cells following acute exposure to 200 mg/mL of the organophosphate insecticide, malathion for 6 and 24 hours. Metabolite compounds are listed by their chemical class. Fold changes in relative abundance from control and the associated P values are given for both 6 hour and 24 hour exposure times. Compound information includes but is not limited to retention time (RT (min)), retention index (RI), relative standard deviation of the average RI (RI RSD (%)), base peak mass/es (BP *m/z* (EI)) and compound identification parameters. Each compound is given an ID score based on a scale of identification criteria as proposed by Abbiss et al (2015). Table headings are defined as below the table.

TOP

A

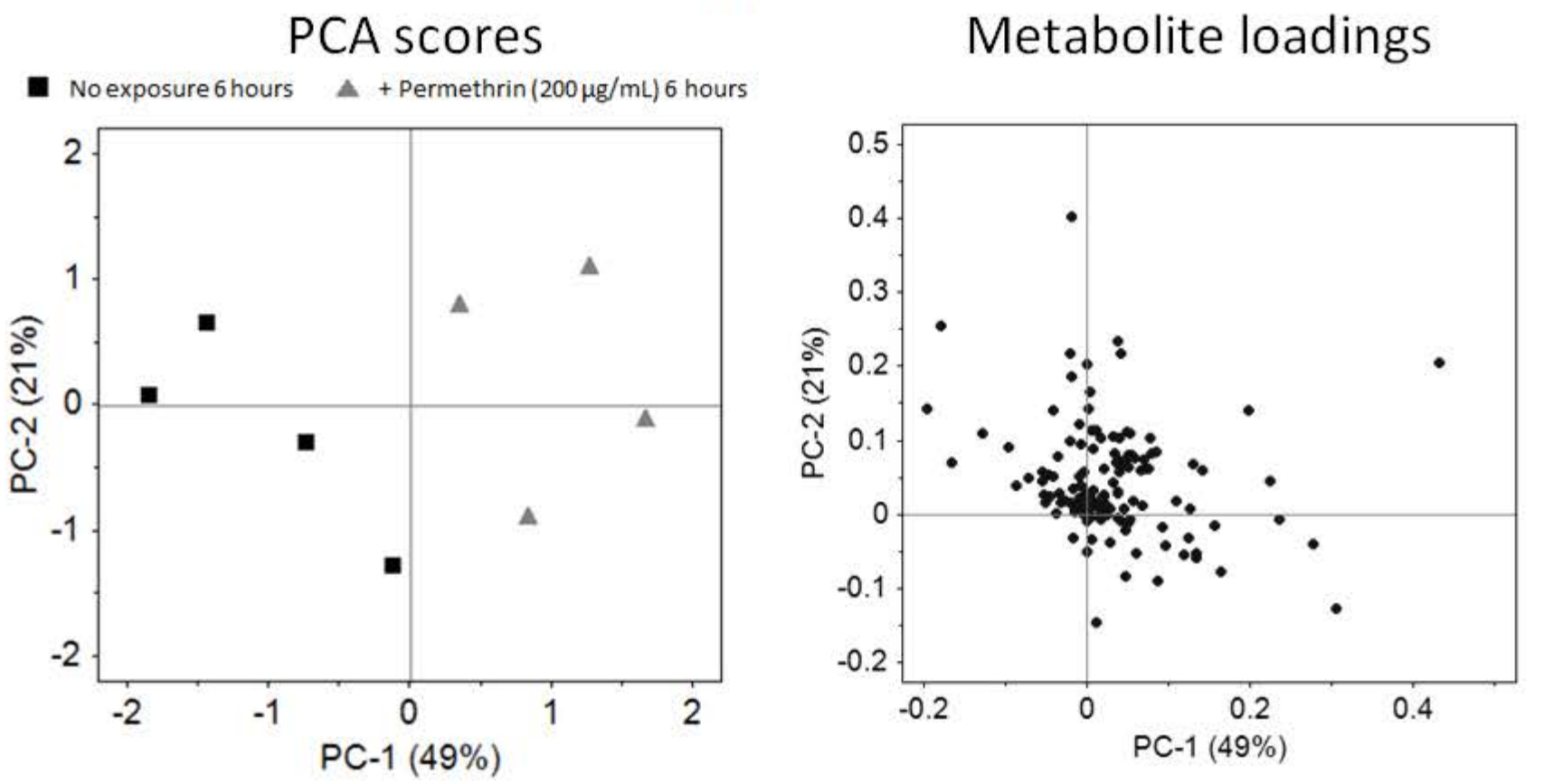
PCA scores
Metabolite loadings
No exposure 6 hours
+ Permethrin (200 µg/mL) 6 hours
PC-2 (21%)
PC-1 (49%)
PC-2 (21%)
PC-1 (49%)

B

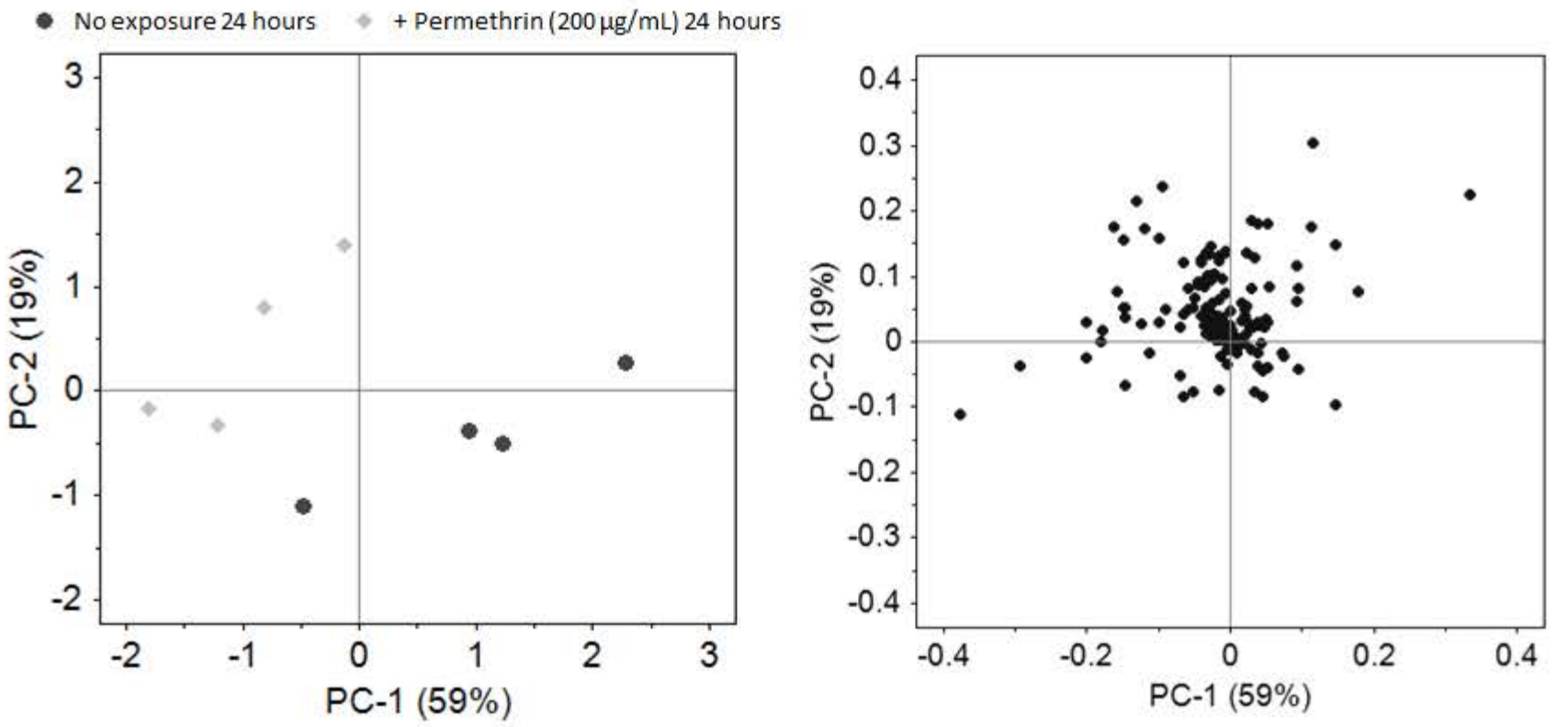
No exposure 24 hours
+ Permethrin (200 µg/mL) 24 hours
PC-2 (19%)
PC-1 (59%)
PC-2 (19%)
PC-1 (59%)

C

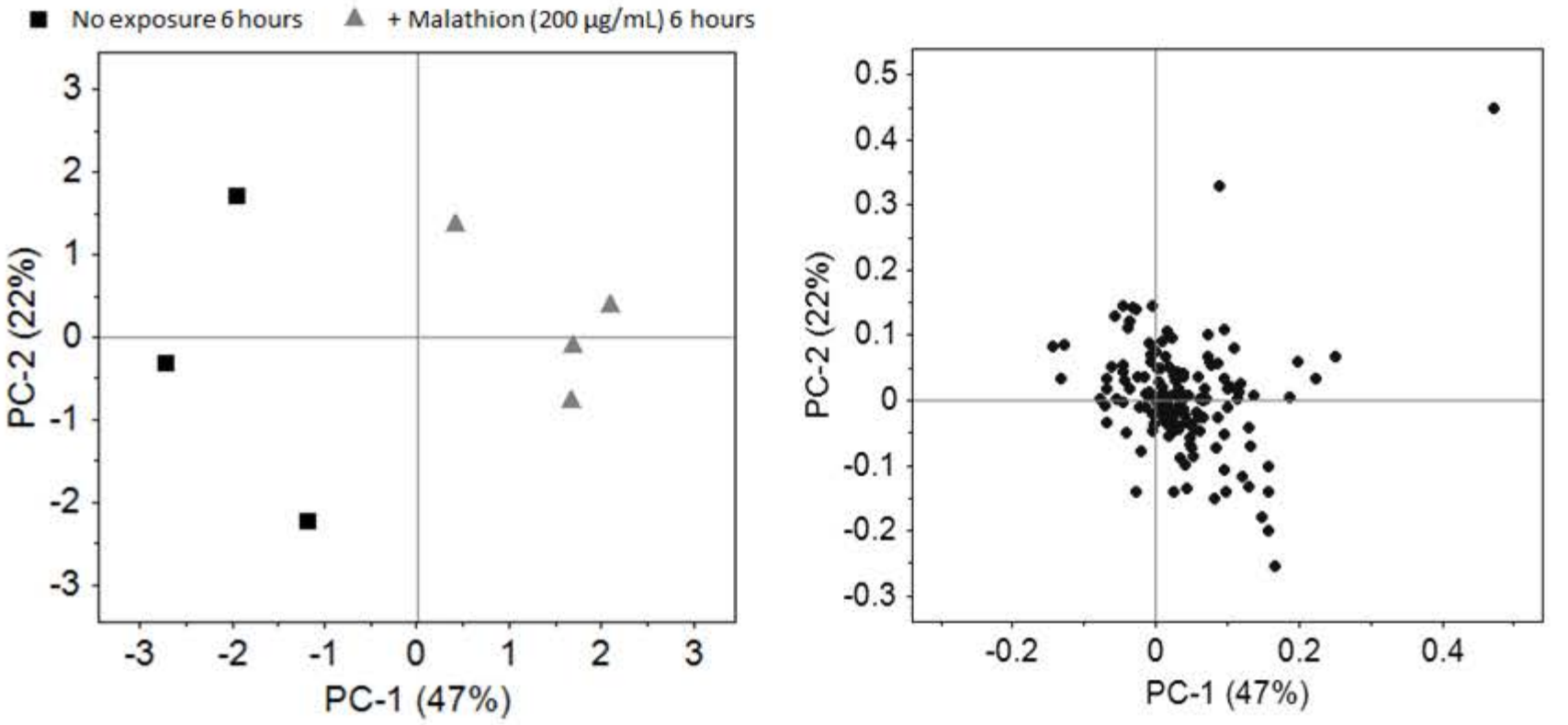
No exposure 6 hours
+ Malathion (200 µg/mL) 6 hours
PC-2 (22%)
PC-1 (47%)
PC-2 (22%)
PC-1 (47%)

D

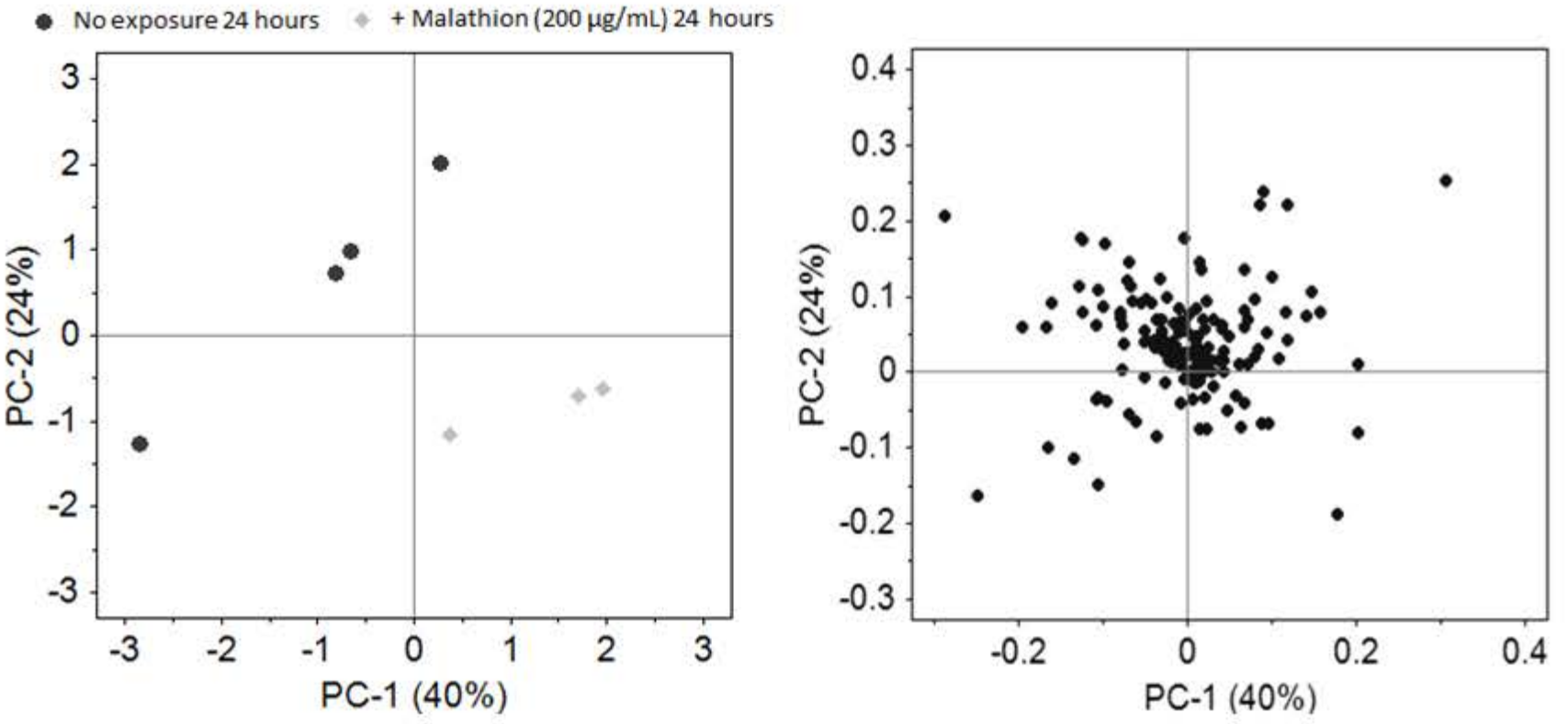
No exposure 24 hours
+ Malathion (200 µg/mL) 24 hours
PC-2 (24%)
PC-1 (40%)
PC-2 (24%)
PC-1 (40%)

TOP

+ Permethrin (200 µg/mL)

+ Malathion (200 µg/mL)

Carbohydrates

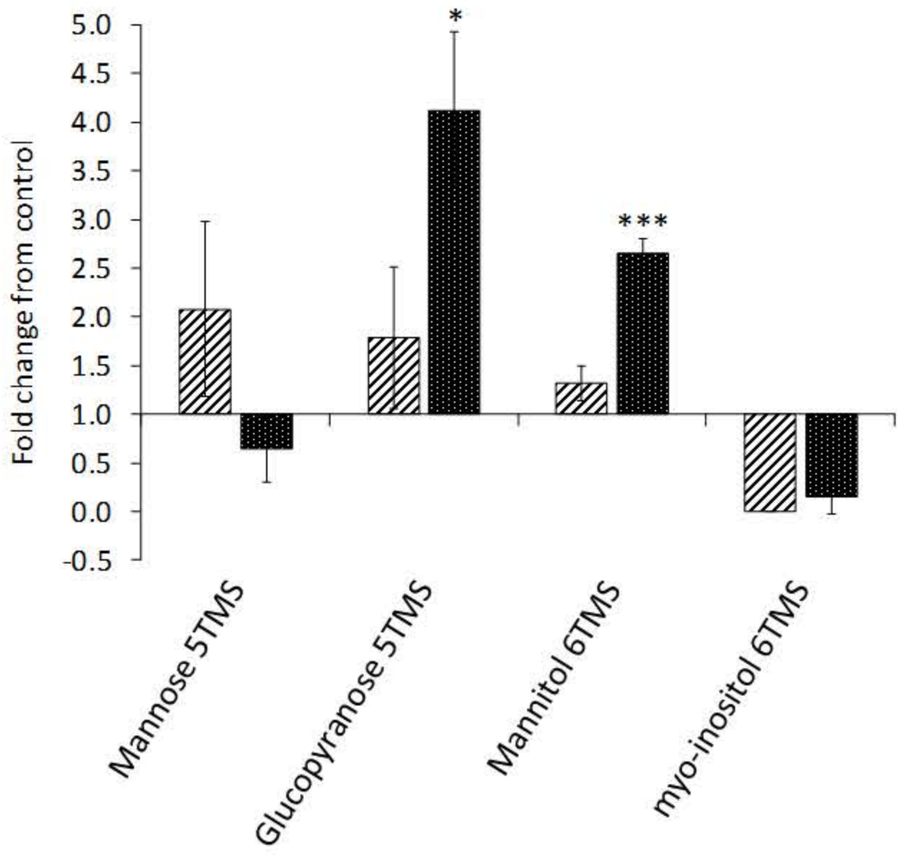

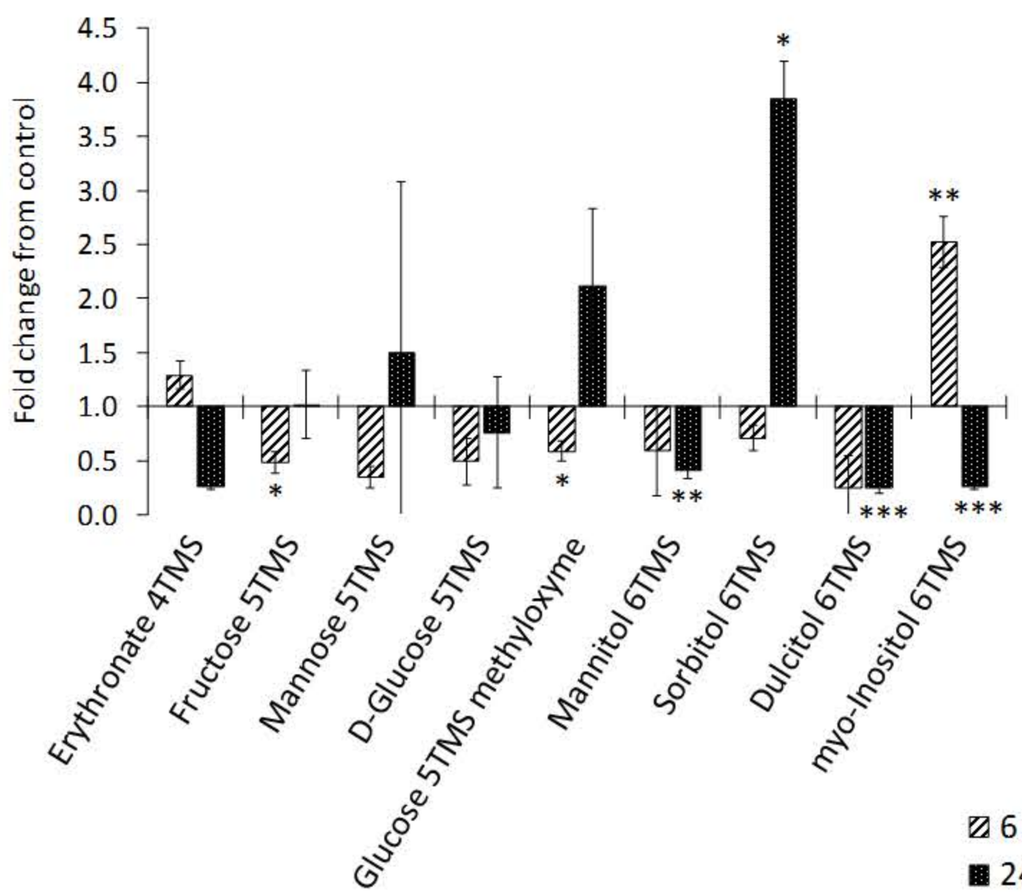

Others

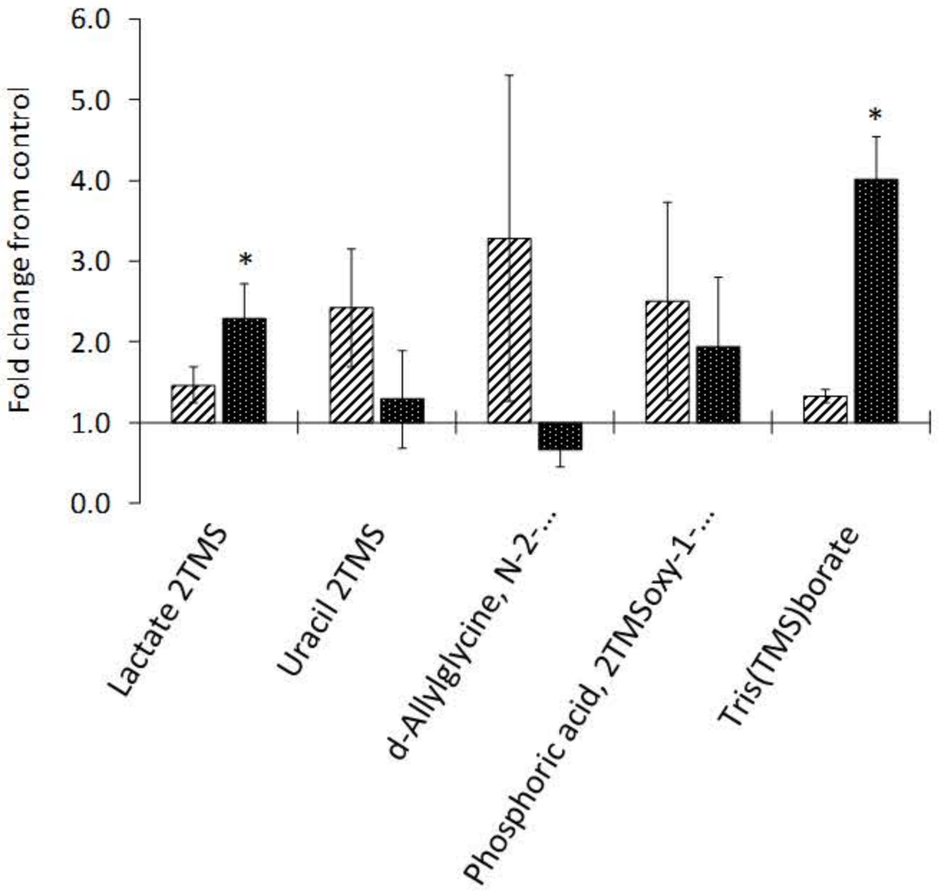

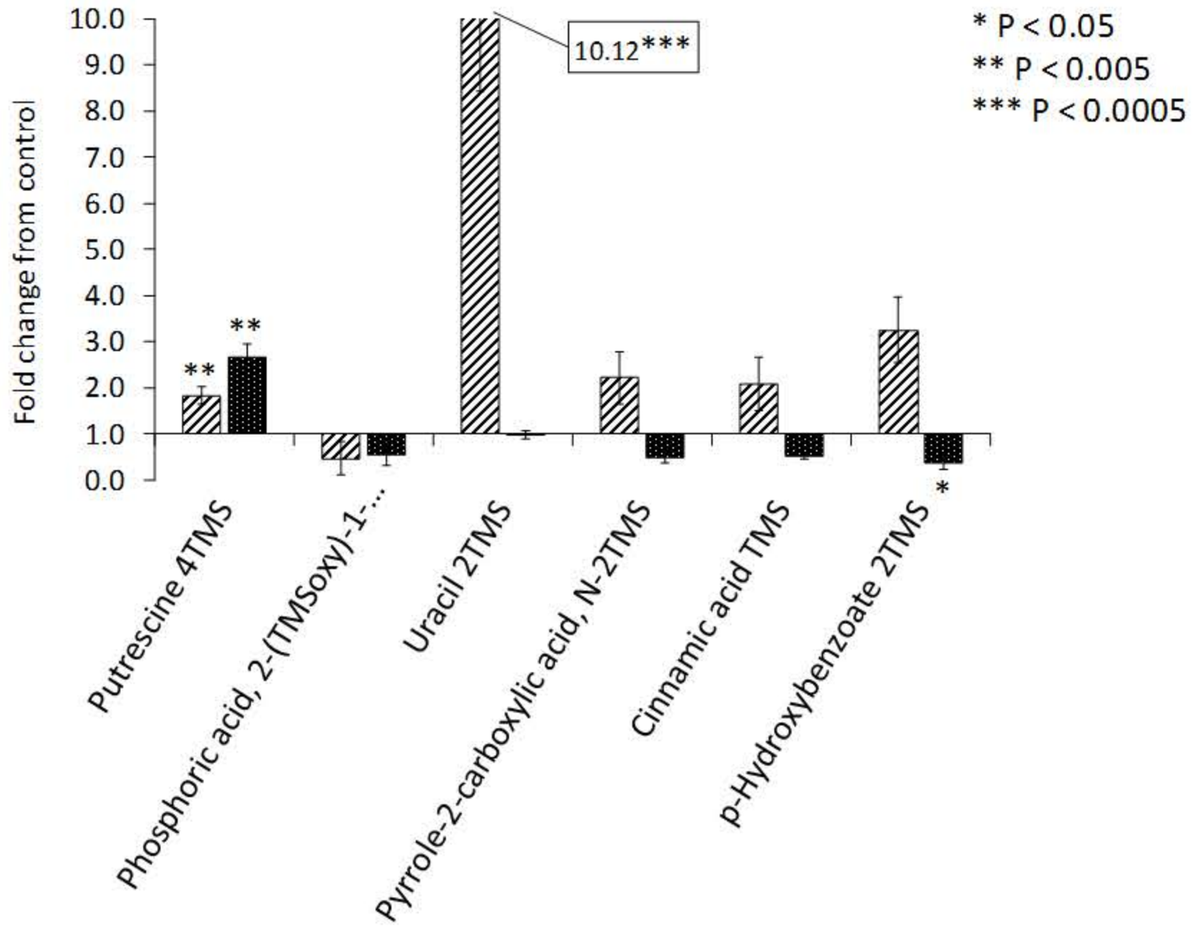

Unknowns
+ Permethrin
(200 µg/mL)

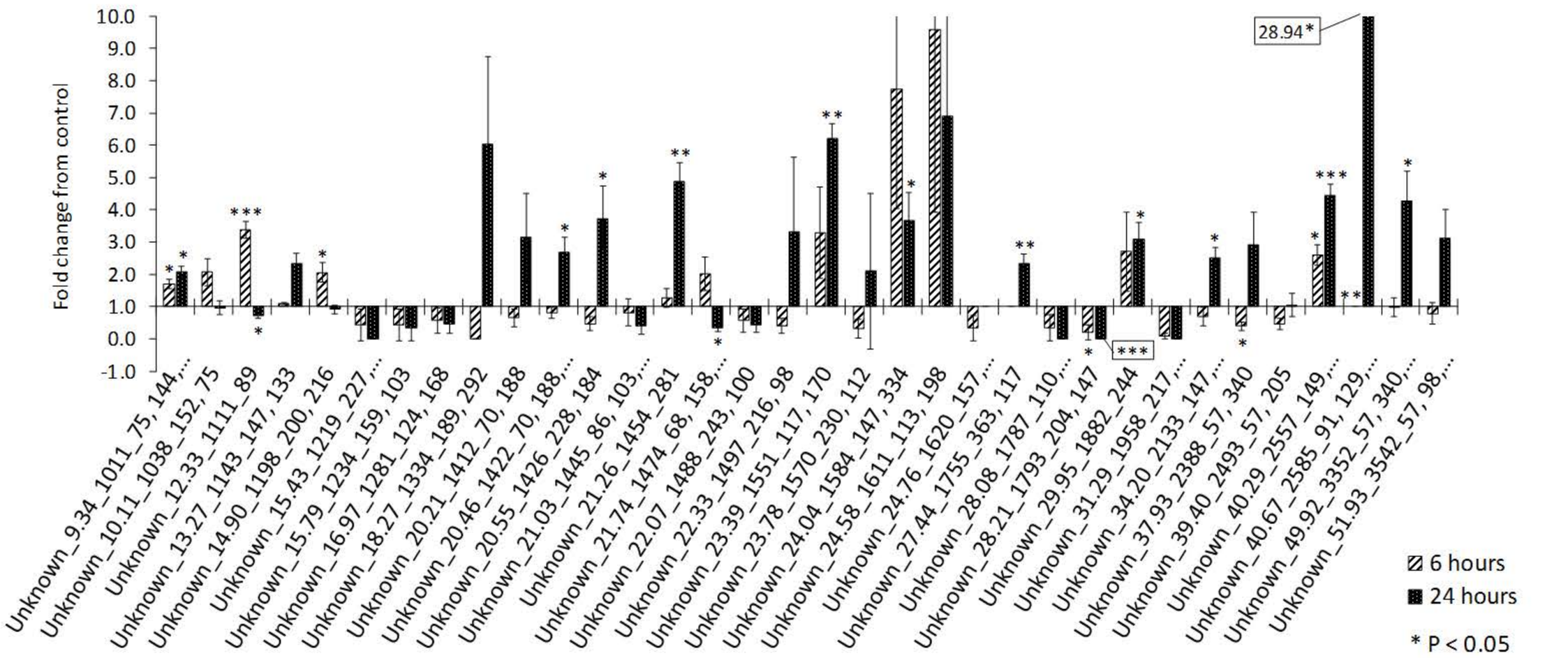

Unknowns
+ Malathion
(200 µg/mL)

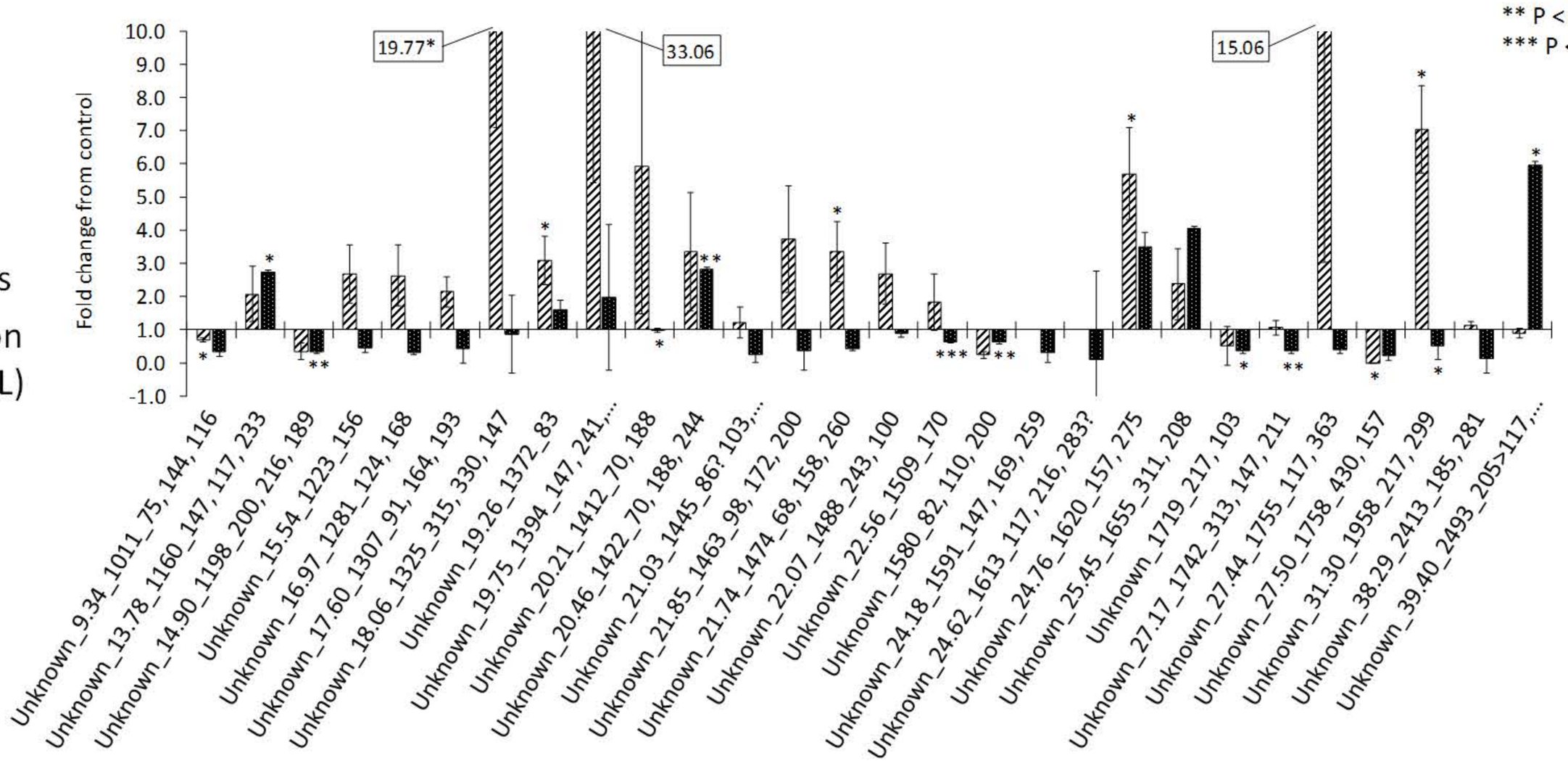

Supplementary Information Table S1

Intracellular metabolites of B50 cells following acute exposure to 200 mg/mL of the pyrethroid insecticide, permethrin for 6 and 24 hours. Metabolite compounds are listed by their chemical class. Fold changes in relative abundance from control and the associated P values are given for both 6 hour and 24 hour exposure times. Compound information includes but is not limited to retention time (RT (min)), retention index (RI), relative standard deviation of the average RI (RI RSD (%)), base peak mass/es (BP *m/z* (EI)) and compound identification parameters. Each compound is given an ID score based on a scale of identification criteria as proposed by Abbiss et al 2015. Table headings are defined as below the table.

Compounds detected, listed by chemical class	Fold change 6 hrs (± SE)	P value 6 hrs	Fold change 24 hrs (± SE)	P value 24 hrs	RT (min)	RI	RI RSD (%)	BP *m/z* (EI)	User library match	NIST match	NIST probability (%)	Detected in samples (%)	ID Score
Alpha hydroxy acids													
Lactate 2TMS	1.47 ± 0.225	0.11078	2.29 ± 0.424	0.03390	10.93	1060	0.14	147	✓	✓	91.2	100	7
Amino acids													
L-Alanine 2TMS	1.38 ± 0.044	0.01957	0.87 ± 0.131	0.36123	11.87	1101	0.10	116	✓	-	62.7	100	5
L-Valine TMS	1.54 ± 0.148	0.01108	1.62 ± 0.280	0.04197	11.92	1103	0.16	72	✓	✓	89.2	100	7
L-Valine 2TMS	1.35 ± 0.070	0.02720	1.52 ± 0.099	0.00768	15.21	1211	0.05	144	✓	✓	81.6	100	7
L-Leucine TMS	1.51 ± 0.133	0.00812	1.56 ± 0.244	0.03974	13.74	1162	0.32	86	✓	✓	90.3	100	7
L-Leucine 2TMS	1.80 ± 0.321	0.07792	2.20 ± 0.549	0.10667	16.74	1273	0.00	158	✓	✓	86.2	100	7
L-Isoleucine TMS	1.79 ± 0.199	0.00572	1.79 ± 0.215	0.01176	14.34	1181	0.24	86	✓	✓	81.3	100	7
L-Isoleucine 2TMS	1.38 ± 0.041	0.03863	1.53 ± 0.083	0.00418	17.29	1295	0.07	158	✓	✓	81.8	100	7
L-Serine 2TMS	1.66 ± 0.132	0.00224	1.53 ± 0.192	0.02139	16.38	1258	0.17	132	✓	✓	98.0	100	7
L-Serine 3TMS	1.23 ± 0.080	0.19375	1.79 ± 0.240	0.01719	18.99	1363	0.03	204	✓	✓	88.7	100	7
L-Threonine 2TMS	1.64 ± 0.134	0.00254	0.94 ± 0.099	0.55818	17.44	1301	0.13	117	✓	✓	91.6	100	7
L-Threonine 3TMS	1.46 ± 0.083	0.02484	1.17 ± 0.146	0.32655	19.60	1387	0.07	218	✓	✓	97.9	100	7
L-Glycine 3TMS	1.56 ± 0.090	0.00091	1.57 ± 0.155	0.00573	17.61	1308	0.01	174	✓	✓	90.3	100	7
L-Methionine TMS	1.50 ± 0.129	0.01142	1.15 ± 0.080	0.26720	20.36	1418	0.02	104	✓	✓	89.7	100	7
L-Methionine 2TMS	0.26 ± 0.096	0.43445	1.41 ± 0.788	0.73039	22.71	1515	0.03	176	✓	✓	93.7	95	7
L-Aspartate 3TMS	1.48 ± 0.071	0.21451	2.60 ± 0.398	0.00396	21.61	1468	0.06	232	✓	-	54.3	100	5
L-Aspartate 3TMS	1.26 ± 0.466	0.77225	0.40 ± 0.258	0.18417	22.72	1516	0.04	232	✓	-	-	100	5
Pyroglutamate 2TMS	1.49 ± 0.177	0.03525	2.08 ± 0.168	0.01549	22.97	1528	0.09	156	✓	✓	94.6	100	7
L-Glutamate TMS	1.62 ± 0.205	0.03120	1.70 ± 0.064	0.06546	23.05	1532	0.13	84	✓	-	53.9	100	5

L-Glutamate 3TMS	0.71 ± 0.247	0.91969	0.17 ± 0.101	0.00536	24.85	1623	0.03	246	✓	✓	91.9	90	7
L-Proline 2TMS	0.46 ± 0.191	0.32403	0.43 ± 0.315	0.19931	23.92	1580	0.23	142	✓	-	-	80	5
2-Aminobutyric acid 2TMS	0.42 ± 0.177	0.12658	0.50 ± 0.332	0.20561	14.10	1171	0.05	130	-	✓	81.9	85	3
Polyamines													
Putrescine 4TMS	1.46 ± 0.084	0.00683	1.58 ± 0.396	0.15778	27.11	1739	0.11	174	-	✓	89.9	100	3
Benzenoids/Acetophenones/ Benzyl alcohols													
Acetophenone	↑	0.00000	-	-	11.40	1081	0.00	105	-	✓	95.9	20	3
Benzoate TMS	↑	0.39100	↑	0.00058	16.33	1256	0.22	179	✓	✓	92.5	85	7
4-Piperidyl benzilate	↑	0.06105	-	-	41.77	2665	0.00	183	-	✓	85.4	15	3
Dicarboxylic acids													
Succinate 2TMS	2.11 ± 0.380	0.04929	1.71 ± 0.121	0.01621	17.89	1319	0.04	147	✓	✓	90.0	100	7
Fumarate TMS	2.50 ± 0.504	0.10283	1.32 ± 0.219	0.39027	18.84	1357	0.05	245	✓	-	67.9	95	5
Glutarate 2TMS	3.21 ± 0.759	0.03139	1.26 ± 0.312	0.46049	20.10	1408	0.07	147	✓	✓	81.0	95	7
Malate 3TMS	2.03 ± 0.152	0.06387	2.40 ± 0.292	0.01160	22.01	1484	0.01	147	✓	✓	91.3	100	7
Keto acids													
2-Oxoglutarate 2TMS	1.97 ± 0.507	0.19504	1.13 ± 0.243	0.65675	24.04	1582	0.03	147	✓	-	-	90	5
Pyruvate 2TMS	0.13 ± 0.065	0.10724	0.62 ± 0.326	0.68416	11.63	1088	0.03	147	-	✓	88.4	90	3
Hydroxy fatty acids													
2-Hydroxyisovaleric acid 2TMS	0.75 ± 0.175	0.19672	1.41 ± 0.128	0.03517	14.81	1195	0.04	147	-	✓	83.6	100	3
3-Hydroxyisovaleric acid 2TMS	-	-	↓	0.00845	15.15	1208	0.02	131	-	✓	80.3	20	3
Long-chain fatty acids													
Tetradecanoic acid (Myristic acid) TMS	2.67 ± 0.964	0.09507	1.90 ± 0.224	0.01235	29.34	1850	0.03	117	-	✓	90.6	100	3
Pentadecanoic acid TMS	3.10 ± 1.360	0.16343	2.69 ± 0.575	0.03675	31.11	1943	0.06	299	-	✓	92.1	95	3
Palmitelaidic acid TMS	3.39 ± 2.234	0.30959	1.96 ± 1.127	0.41996	32.33	2021	0.05	75	-	✓	82.6	85	3
Palmitelaidic acid TMS	3.87 ± 1.636	0.06435	2.61 ± 1.023	0.12705	32.42	2026	0.04	75	-	✓	88.0	95	3
Hexdecanoate (Palmitic acid) TMS	2.88 ± 0.890	0.03544	2.21 ± 0.317	0.07632	32.83	2048	0.05	117	✓	✓	95.3	100	7
Octadecenoate (Oleic acid) TMS	3.50 ± 1.491	0.11083	2.62 ± 1.139	0.14278	35.49	2208	0.26	75	✓	✓	89.6	100	7
Oleic acid (cis-9-Octadecenoic acid) TMS	2.32 ± 0.922	0.19384	1.87 ± 0.501	0.23791	35.61	2221	0.01	75	-	✓	85.4	95	3

Octadecanoate (Stearic acid) TMS	3.65 ± 1.163	0.02940	2.68 ± 0.669	0.10122	35.97	2243	0.02	117	✓	✓	87.4	100	7
Cholesterols													
Cholesterol TMS	0.35 ± 0.067	0.03091	1.57 ± 0.178	0.13095	47.85	3153	0.16	129	✓	✓	89.5	100	7
Organic phosphoric acids													
Ethyl phosphoric acid 2TMS	-	-	↑	0.00438	15.63	1227	0.01	211	-	✓	91.8	20	3
Pyrimidines													
Uracil 2TMS	2.43 ± 0.732	0.07770	1.29 ± 0.601	0.69877	18.56	1346	0.27	241	✓	✓	80.2	100	7
Peptides													
d-Allylglycine, N-(2-methoxy-ethylcarbonyl)-, heptyl ester	3.28 ± 2.025	0.28049	0.66 ± 0.212	0.21723	23.32	1546	0.01	172	-	✓	80.1	90	3
Monosaccharides													
Mannose 5TMS	2.08 ± 0.894	0.26191	0.64 ± 0.339	0.57052	29.85	1874	0.05	319	✓	✓	85.0	100	7
Glucose 5TMS	1.41 ± 0.078	0.00391	0.89 ± 0.047	0.34521	30.21	1884	0.08	319	✓	✓	87.0	100	7
Glucose 5TMS	1.26 ± 0.149	0.16037	0.57 ± 0.077	0.14545	30.39	1902	0.01	319	✓	✓	90.9	100	7
Glucopyranose 5TMS	1.78 ± 0.724	0.30309	4.13 ± 0.797	0.01073	31.49	1967	0.23	204	✓	✓	85.0	100	7
Unidentified carbohydrate 4TMS	0.04 ± 0.052	0.10765	1.23 ± 0.872	0.82388	31.96	1998	0.01	217	✓	-	-	60	0.5
Sugar alcohols													
Ribitol (Adonitol) 5TMS	1.50 ± 0.103	0.00331	1.82 ± 0.218	0.00651	26.84	1723	0.01	217	✓	✓	88.5	100	7
Mannitol 6TMS	1.32 ± 0.175	0.15297	2.65 ± 0.157	0.00011	30.59	1914	0.07	319	✓	-	54.4	100	5
Sorbitol 6TMS	↓	0.39100	↑	0.14641	30.71	1921	0.04	319	✓	-	52.6	25	5
Cyclic alcohols													
myo-inositol 6TMS	↓	0.39100	0.15 ± 0.172	0.08516	32.32	2017	0.00	318	✓	-	64.6	30	5
myo-Inositol 6TMS	1.81 ± 0.164	0.00478	0.90 ± 0.079	0.32230	33.36	2080	0.01	217	✓	✓	92.4	100	7
Non-metal phosphates													
Phosphoric acid, 2TMSoxy-1-[(TMSoxy)methyl]ethyl 2TMS	2.51 ± 1.227	0.22417	1.95 ± 0.852	0.28538	26.92	1728	0.02	243	-	✓	93.2	100	3
Inorganics													
Tris(TMS)borate	1.32 ± 0.084	0.12359	4.01 ± 0.536	0.00017	8.37	979	0.12	221	-	✓	94.7	100	3
Miscellaneous													
N-TMS methoxyamine ARTEF	1.05 ± 0.063	0.61904	1.87 ± 0.320	0.02945	9.84	1025	0.06	119	-	✓	80.8	100	3

Pentasiloxane, dodecamethyl- ARTEF	1.07 ± 0.111	0.62781	1.42 ± 0.174	0.04183	13.88	1164	0.07	147	-	✓	91.2	100	3
Cyclohexasiloxane, dodecamethyl- ARTEF	2.09 ± 0.570	0.11158	1.03 ± 0.499	0.96146	17.56	1305	0.02	341	-	✓	95.9	95	3
MSTFA ARTEF	0.65 ± 0.307	0.22028	2.96 ± 0.730	0.04883	18.34	1337	0.00	184	-	✓	82.9	100	3
Cycloheptasiloxane, tetradecamethyl- ARTEF	2.55 ± 0.777	0.09973	0.52 ± 0.467	0.27217	21.51	1465	0.03	281	-	✓	97.4	90	3
Heptasiloxane, hexadecamethyl- ARTEF	3.65 ± 2.628	0.42136	↓	0.01216	23.20	1542	0.11	221	-	✓	96.9	75	3
Heptasiloxane, hexadecamethyl- ARTEF	1.26 ± 0.705	0.99817	0.28 ± 0.065	0.00404	26.36	1700	0.04	221	-	✓	92.0	100	3
Cyclononasiloxane, octadecamethyl- ARTEF	2.40 ± 1.254	0.42701	0.38 ± 0.042	0.00770	27.97	1781	0.03	429	-	✓	94.4	100	3
Cyclodecasiloxane, eicosamethyl- ARTEF	1.41 ± 0.632	0.66148	0.30 ± 0.045	0.00123	30.62	1918	0.08	281	-	✓	95.0	100	3
Unknowns													
Unknown_9.34_1011	1.70 ± 0.146	0.01884	2.08 ± 0.183	0.01475	9.34	1011	0.04	75, 144, 116	-	-	-	100	0
Unknown_10.11_1038	2.07 ± 0.421	0.04471	0.97 ± 0.224	0.95456	10.11	1038	0.00	152, 75	-	-	-	100	0
Unknown_12.33_1111	3.37 ± 0.260	0.00032	0.73 ± 0.093	0.32047	12.33	1111	0.01	89	-	-	-	100	0
Unknown_13.27_1143	1.10 ± 0.020	0.34533	2.34 ± 0.307	0.00633	13.27	1143	0.07	147, 133	-	-	-	100	0
Unknown_14.90_1198	2.06 ± 0.294	0.01247	0.91 ± 0.118	0.68797	14.90	1198	0.04	200, 116	-	-	-	100	0
Unknown_15.37_1216	↑	0.00080	-	-	15.37	1216	0.00	193, 75	-	-	-	20	0
Unknown_15.43_1219	0.43 ± 0.501	0.42661	↓	0.05534	15.43	1219	0.04	227, 212, 139	-	-	-	45	0
Unknown_15.45_1220	↑	0.06377	↑	0.12062	15.45	1220	0.00	147, 103, 227	-	-	-	35	0
Unknown_15.79_1234	0.43 ± 0.498	0.39406	0.35 ± 0.398	0.26933	15.79	1234	0.05	159, 103	-	-	-	55	0
Unknown_16.09_1246	1.19 ± 0.312	0.59809	1.89 ± 0.431	0.07189	16.09	1246	0.01	191, 184	-	-	-	100	0
Unknown_16.13_1247	↑	0.07560	↑	0.39100	16.13	1247	0.05	100, 144	-	-	-	25	0
Unknown_16.97_1281	0.58 ± 0.388	0.53209	0.46 ± 0.286	0.36391	16.97	1281	0.02	124, 168	-	-	-	100	0
Unknown_18.27_1334	-	-	6.03 ± 2.713	0.11906	18.27	1334	0.00	189, 292	-	-	-	20	0
Unknown_19.26_1372	1.24 ± 0.616	0.80774	0.51 ± 0.253	0.26135	19.26	1372	0.03	83	-	-	-	100	0
Unknown_19.47_1382	1.31 ± 1.516	0.98287	↑	0.07541	19.47	1382	0.00	129, 144	-	-	-	50	0
Unknown_20.21_1412	0.65 ± 0.272	0.71795	3.14 ± 1.351	0.14018	20.21	1412	0.04	70, 188	-	-	-	100	0
Unknown_20.46_1422	0.81 ± 0.181	0.81891	2.70 ± 0.455	0.01144	20.46	1422	0.02	70, 188, 244	-	-	-	100	0
Unknown_20.55_1426	0.47 ± 0.212	0.12060	3.74 ± 0.985	0.04485	20.55	1426	0.02	228, 184	-	-	-	100	0

Unknown_21.03_1445	0.81 ± 0.415	0.67907	0.40 ± 0.247	0.21441	21.03	1445	0.00	86, 103, 147, 247	-	-	-	85	0
Unknown_21.26_1454	1.26 ± 0.288	0.48519	4.87 ± 0.581	0.00138	21.26	1454	0.01	281	-	-	-	95	0
Unknown_21.74_1474	2.02 ± 0.526	0.08655	0.34 ± 0.102	0.00491	21.74	1474	0.02	68, 158, 260	-	-	-	100	0
Unknown_22.07_1488	0.57 ± 0.353	0.61913	0.43 ± 0.221	0.24214	22.07	1488	0.09	243, 100	-	-	-	100	0
Unknown_22.33_1497	0.41 ± 0.221	0.32901	3.33 ± 2.289	0.35317	22.33	1497	0.03	216, 98	-	-	-	95	0
Unknown_23.39_1551	3.30 ± 1.415	0.16618	6.21 ± 0.457	0.00001	23.39	1551	0.03	117, 170	-	-	-	80	0
Unknown_23.78_1570	0.32 ± 0.293	0.36855	2.09 ± 2.417	0.69312	23.78	1570	0.01	230, 112	-	-	-	60	0
Unknown_24.04_1584	7.74 ± 3.702	0.12146	3.65 ± 0.876	0.03089	24.04	1584	0.01	147, 334	-	-	-	60	0
Unknown_24.58_1611	9.58 ± 5.670	0.15400	6.90 ± 3.520	0.10564	24.58	1611	0.03	113, 198	-	-	-	45	0
Unknown_24.62_1613	-	-	↑	0.05790	24.62	1613	0.01	117, 216, 283	-	-	-	20	0
Unknown_24.76_1620	0.33 ± 0.384	0.20662	↑	0.39100	24.76	1620	0.01	157, 246, 275	-	-	-	30	0
Unknown_24.98_1631	-	-	↑	0.03625	24.98	1631	0.00	174, 355	-	-	-	20	0
Unknown_25.45_1655	1.99 ± 0.822	0.31495	0.66 ± 0.575	0.68146	25.45	1655	0.03	311, 208	-	-	-	90	0
Unknown_26.08_1686	-	-	↑	0.00273	26.08	1686	0.01	117, 230, 186	-	-	-	20	0
Unknown_27.17_1742	1.97 ± 0.165	0.00958	1.61 ± 0.198	0.02461	27.17	1742	0.04	313, 147, 211	-	-	-	80	0
Unknown_27.44_1755	↑	0.39100	2.34 ± 0.273	0.00274	27.44	1755	0.03	363, 117	-	-	-	45	0
Unknown_28.08_1787	0.35 ± 0.403	0.31098	-	-	28.08	1787	0.01	110, 242, 138	-	-	-	25	0
Unknown_28.21_1793	0.20 ± 0.233	0.02070	↓	0.00014	28.21	1793	0.01	204, 147	-	-	-	45	0
Unknown_28.32_1800	↑	0.39100	↑	0.01937	28.32	1800	0.00	217, 129	-	-	-	25	0
Unknown_28.50_1808	-	-	↑	0.01281	28.50	1808	0.00	217, 437	-	-	-	20	0
Unknown_28.56_1811	↑	0.39100	↑	0.00827	28.56	1811	0.00	204, 437	-	-	-	25	0
Unknown_29.95_1882	2.70 ± 1.218	0.17815	3.09 ± 0.531	0.00803	29.95	1882	0.04	244	-	-	-	90	0
Unknown_31.29_1958	0.08 ± 0.097	0.17123	↓	0.06868	31.29	1958	0.01	217, 299, 129	-	-	-	45	0
Unknown_34.20_2133	0.70 ± 0.291	0.32930	2.51 ± 0.329	0.02791	34.20	2133	0.05	147, 221, 295	-	-	-	80	0
Unknown_34.87_2173	0.96 ± 0.084	0.96105	1.56 ± 0.141	0.01572	34.87	2173	0.07	57, 281	-	-	-	100	0
Unknown_37.93_2388	0.40 ± 0.123	0.01732	2.92 ± 1.010	0.10591	37.93	2388	0.06	57, 340	-	-	-	100	0
Unknown_39.40_2493	0.46 ± 0.182	0.11719	1.05 ± 0.356	0.75942	39.40	2493	0.05	57, 205	-	-	-	85	0
Unknown_40.29_2557	2.60 ± 0.326	0.00761	4.46 ± 0.338	0.00039	40.29	2557	0.03	149, 167, 57	-	-	-	90	0
Unknown_40.47_2571	↑	0.00060	↑	0.03121	40.47	2571	0.00	91, 129, 207	-	-	-	40	0

Unknown_40.64_2583	0.50 ± 0.142	0.03578	1.99 ± 0.377	0.04356	40.64	2583	0.09	57, 98, 120, 340	-	-	-	100	0
Unknown_40.67_2585	↑	0.00127	28.94 ± 8.145	0.02090	40.67	2585	0.01	91, 129, 207	-	-	-	45	0
Unknown_43.14_2763	0.62 ± 0.170	0.11394	2.31 ± 0.362	0.01210	43.14	2763	0.06	57, 98, 120, 340	-	-	-	100	0
Unknown_45.56_2964	0.63 ± 0.173	0.10548	2.41 ± 0.371	0.01107	45.56	2964	0.06	57, 98, 120, 340	-	-	-	100	0
Unknown_49.92_3352	0.97 ± 0.284	0.91080	4.28 ± 0.903	0.01337	49.92	3352	0.02	57, 340, 424	-	-	-	90	0
Unknown_51.93_3542	0.79 ± 0.338	0.62156	3.12 ± 0.881	0.06384	51.93	3542	0.01	57, 98, 120, 340	-	-	-	95	0

Table heading definitions:

Compounds detected	Name of the compound and its derivatisation groups (TMS = trimethylsilyl).
Fold change (± SE)	Fold change in the average metabolite relative abundance from control to permethrin-exposed cells after 6 and 24 hours, ± standard error (SE) of the mean. ↑ = increased from below the limit of detection, ↓ = decreased to below the limit of detection, and no entry indicates the feature was undetectable in all samples at that time point.
P value	P values for 6 and 24 hours metabolite fold changes, calculated using a two-tailed Student's t test between the control and treatment groups per time point, of each metabolite feature using $\log_{10}(X + 1)$ transformed, normalised relative abundances. Data were considered non-normally distributed with unequal variances.
RT (min)	Average measured retention time in minutes.
RI	Average calculated retention index.
RI RSD (%)	Relative standard deviation of the average calculated retention index.
BP *m/z* (EI)	Deconvoluted base peak (or extracted ion) mass/es (EI = electron ionisation).
User library match	Indicates whether a compound was matched to a user-generated library of authentic metabolite standards.
NIST match	Indicates compounds confidently matched to NIST database with probability >80%.
NIST probability (%)	Average calculated NIST probability score for a NIST matched compound.
Detected in samples (%)	Proportion of samples (as a percentage) in which the compound was detected.
ID Score	Compound identification score based on the proposed identification scoring system outlined in Abbiss et al 2015: 7 = Match to authentic standard + RT ± 2.5% + confident NIST match 5 = Match to authentic standard + RT ± 2.5% 3 = Confident NIST match + RT ± 2.5% 1.5 = Confident NIST match 0.5 = Compound class match 0 = Unknown

Supplementary Information Table S2

Intracellular metabolites of B50 cells following acute exposure to 200 mg/mL of the organophosphate insecticide, malathion for 6 and 24 hours. Metabolite compounds are listed by their chemical class. Fold changes in relative abundance from control and the associated P values are given for both 6 hour and 24 hour exposure times. Compound information includes but is not limited to retention time (RT (min)), retention index (RI), relative standard deviation of the average RI (RI RSD (%)), base peak mass/es (BP *m/z* (EI)) and compound identification parameters. Each compound is given an ID score based on a scale of identification criteria as proposed by Abbiss et al 2015. Table headings are defined as below the table.

Compounds detected, listed by chemical class	Fold change 6 hrs (± SE)	P value 6 hrs	Fold change 24 hrs (± SE)	P value 24 hrs	RT (min)	RI	RI RSD (%)	BP *m/z* (EI)	User library match	NIST match	NIST probability (%)	Detected in samples (%)	ID Score
Amino acids													
L-Alanine, N-(trifluoroacetyl)-TMS	1.33 ± 0.673	0.76308	0.53 ± 0.396	0.32932	11.46	1082	0.00	121	-	✓	83.1	94	3
L-Alanine 2TMS	1.65 ± 0.233	0.03597	0.26 ± 0.017	0.00029	11.87	1101	0.10	116	✓	✓	83.7	100	7
L-Alanine 3TMS	1.93 ± 0.683	0.22027	0.39 ± 0.069	0.02799	20.08	1407	0.00	116	✓	-	-	100	5
L-Aspartate 3TMS	1.66 ± 0.197	0.08396	0.35 ± 0.070	0.00086	21.61	1468	0.00	232	✓	-	58.8	100	5
L-Glutamate TMS	1.20 ± 0.176	0.44235	0.49 ± 0.151	0.07512	23.05	1532	0.13	84	✓	-	61.9	100	5
2-Pyrrolidone-5-carboxylic acid (Pyroglutamate) TMS	2.12 ± 0.790	0.30055	0.61 ± 0.219	0.85927	22.65	1511	0.03	84	-	✓	89.9	100	3
Pyroglutamate 2TMS	13.81 ± 6.891	0.09329	0.95 ± 0.420	0.60235	22.79	1519	0.02	156	✓	-	58.8	83	5
Pyroglutamate 2TMS	0.60 ± 0.358	0.25535	0.99 ± 0.225	0.84825	22.97	1528	0.09	156	✓	-	-	100	5
L-Glycine 2TMS	1.48 ± 0.427	0.27934	0.31 ± 0.047	0.00195	12.54	1123	0.05	102	✓	✓	84.3	100	7
L-Glycine 3TMS	1.03 ± 0.014	0.31193	0.91 ± 0.004	0.00650	17.61	1308	0.09	174	✓	✓	89.1	100	7
L-Isoleucine TMS	2.83 ± 0.450	0.00368	1.08 ± 0.077	0.54619	14.34	1181	0.24	86	✓	-	74.4	100	5
L-Isoleucine 2TMS	3.63 ± 0.666	0.00264	0.98 ± 0.008	0.86873	17.29	1295	0.07	158	✓	-	60.8	100	5
L-Leucine TMS	2.37 ± 0.501	0.02037	1.11 ± 0.091	0.46904	13.74	1162	0.32	86	✓	✓	85.5	100	7
L-Leucine 2TMS	1.90 ± 0.419	0.06713	0.88 ± 0.031	0.60361	16.74	1273	0.01	158	✓	-	73.1	100	5
L-Methionine TMS	1.24 ± 0.045	0.00389	0.93 ± 0.022	0.05357	20.36	1418	0.02	104	✓	-	70.2	100	5
L-Methionine 2TMS	4.99 ± 1.138	0.06547	1.58 ± 0.414	0.20801	22.71	1515	0.03	176	✓	✓	95.5	94	7
L-Phenylalanine TMS	1.96 ± 0.257	0.01186	0.92 ± 0.041	0.74738	23.40	1550	0.25	120	✓	✓	94.3	100	7
L-Proline TMS	1.71 ± 0.313	0.04578	0.46 ± 0.049	0.00212	14.28	1178	0.04	70	-	✓	87.0	100	3
L-Proline 2TMS	0.81 ± 0.083	0.24607	0.81 ± 0.021	0.00732	17.41	1300	0.00	142	✓	✓	86.0	100	7

L-Proline 2TMS	3.50 ± 1.867	0.24890	0.58 ± 0.117	0.36392	23.92	1580	0.23	142	✓	-	59.6	89	5
L-Serine 2TMS	1.78 ± 0.442	0.07823	2.06 ± 0.176	0.02175	16.38	1258	0.17	132	✓	✓	98.2	100	7
L-Serine 3TMS	2.22 ± 0.265	0.06394	1.45 ± 0.061	0.18227	18.99	1363	0.10	204	✓	✓	92.4	100	7
L-Threonine 2TMS	2.04 ± 0.779	0.26632	0.41 ± 0.146	0.05071	17.44	1301	0.13	117	✓	✓	89.8	100	7
L-Threonine 3TMS	2.33 ± 0.256	0.00382	0.44 ± 0.022	0.00224	19.60	1387	0.07	218	✓	✓	97.8	100	7
L-Valine TMS	2.47 ± 0.731	0.05685	1.26 ± 0.117	0.27764	11.92	1103	0.16	72	✓	✓	86.7	100	7
Aminomalonic acid 3TMS	1.26 ± 0.420	0.68128	0.38 ± 0.191	0.08469	21.56	1467	0.00	147	-	✓	80.9	100	3
Pipecolinic acid TMS	4.29 ± 2.247	0.13512	0.59 ± 0.364	0.63738	16.74	1272	0.00	84	-	✓	87.6	83	3
ß-Alanine 3TMS	0.71 ± 0.030	0.33436	0.38 ± 0.034	0.00049	20.61	1428	0.00	174	✓	✓	91.8	100	7
Polyamines													
Putrescine 4TMS	1.83 ± 0.197	0.00358	2.66 ± 0.292	0.00153	27.11	1739	0.11	174	-	✓	87.2	100	3
Dicarboxylic acids													
Methylsuccinic acid 2TMS	1.62 ± 0.434	0.26374	0.45 ± 0.074	0.02220	18.21	1331	0.03	147	-	✓	83.3	100	3
Succinate 2TMS	1.11 ± 0.276	0.88445	0.42 ± 0.089	0.02306	17.89	1319	0.04	147	✓	✓	87.2	100	7
Fumarate TMS	↓	0.18508	↓	0.03248	18.84	1357	0.01	245	✓	-	-	33	5
Malate 3TMS	0.31 ± 0.284	0.15263	0.08 ± 0.036	0.00389	22.01	1484	0.01	147	✓	✓	84.8	100	7
Keto acids													
Pyruvate 2TMS	1.48 ± 0.284	0.34959	3.35 ± 1.685	0.14919	11.63	1088	0.03	147	-	✓	88.2	94	3
Hydroxy fatty acids													
2-Hydroxybutyric acid 2TMS	1.70 ± 0.736	0.50427	2.72 ± 1.438	0.25276	12.8	1127	0.04	131	-	✓	85.7	78	3
2-Hydroxyisovaleric acid 2TMS	1.13 ± 0.090	0.37377	0.81 ± 0.022	0.01901	14.81	1195	0.04	147	-	✓	89.3	100	3
Long-chain fatty acids													
Oleic acid (cis-9-Octadecenoic acid) TMS	0.91 ± 0.387	0.73557	0.34 ± 0.248	0.41593	35.61	2208	0.01	75	-	✓	88.1	94	3
Organic phosphoric acids													
Ethyl phosphoric acid 2TMS	↑	0.07288	0.51 ± 0.135	0.30597	15.63	1227	0.01	211	-	✓	80.0	56	3
Phosphoric acid, 2-(TMSoxy)-1-[(TMSoxy)methyl] ethyl 2TMS ester	0.47 ± 0.367	0.53002	0.55 ± 0.249	0.39300	26.92	1728	0.02	243	-	✓	81.1	89	3
Pyrimidines													
Uracil 2TMS	10.11 ± 1.678	0.00022	0.98 ± 0.087	0.81293	18.56	1346	0.27	241	✓	✓	89.1	100	7

Carbohydrates													
Erythronate 4TMS	1.29 ± 0.125	0.10546	0.27 ± 0.026	0.00240	23.14	1537	0.02	292	✓	✓	80.0	100	7
Unidentified carbohydrate 5TMS	0.52 ± 0.184	0.38603	1.65 ± 0.161	0.03743	29.11	1839	0.04	103	-	✓	86.7	100	0.5
Monosaccharides													
D-Ribose 4TMS	1.25 ± 0.090	0.03802	0.85 ± 0.200	0.53599	25.97	1679	0.06	103	✓	✓	82.6	100	7
Fructose 5TMS	0.49 ± 0.100	0.01506	1.02 ± 0.313	0.85553	29.59	1861	0.08	103	✓	✓	83.2	100	7
Fructose 5TMS	0.63 ± 0.160	0.21513	0.76 ± 0.201	0.32804	29.77	1870	0.35	103	✓	✓	80.5	100	7
Mannose 5TMS	0.35 ± 0.095	0.16583	1.50 ± 1.586	0.96713	29.85	1874	0.05	319	✓	-	77.5	94	5
Unidentified carbohydrate 2 (NIST D-Glucose 5TMS)	0.49 ± 0.214	0.40362	0.76 ± 0.514	0.85914	30.02	1883	0.01	204	✓	✓	87.6	78	3
Glucose 5TMS	1.17 ± 0.126	0.40175	1.60 ± 0.199	0.05567	30.21	1884	0.08	319	✓	✓	87.8	100	7
Glucose 5TMS	0.59 ± 0.092	0.01858	2.11 ± 0.721	0.08852	30.39	1902	0.01	319	✓	✓	85.7	100	7
Sugar alcohols													
Mannitol 6TMS	0.59 ± 0.411	0.60983	0.41 ± 0.073	0.00238	30.59	1914	0.07	319	✓	-	45.9	78	5
Sorbitol 6TMS	0.71 ± 0.116	0.25480	3.85 ± 0.342	0.00596	30.71	1921	0.04	319	✓	-	55.2	100	5
Dulcitol 6TMS	0.25 ± 0.292	0.29908	0.25 ± 0.053	0.00030	30.80	1926	0.05	217	✓	-	-	61	5
Cyclic alcohols													
myo-Inositol 6TMS	2.53 ± 0.236	0.00097	0.26 ± 0.027	0.00009	33.36	2080	0.01	217	✓	✓	84.7	100	7
Pyrrole carboxylic acids													
Pyrrole-2-carboxylic acid, N-2TMS	2.22 ± 0.566	0.16200	0.49 ± 0.131	0.66038	18.80	1355	0.03	240	-	✓	94.6	100	3
Phenylpropanoic acids													
Hydrocinnamic acid TMS	1.88 ± 0.504	0.30445	1.45 ± 0.544	0.46591	20.50	1424	0.02	104	-	✓	80.0	100	3
Cinnamic acids													
Cinnamic acid TMS	2.08 ± 0.577	0.14647	0.52 ± 0.060	0.25804	23.52	1558	0.03	205	-	✓	81.8	100	3
Benzoic acids													
p-Hydroxybenzoate 2TMS	3.25 ± 0.703	0.05997	0.38 ± 0.138	0.02193	25.07	1634	0.00	267	✓	-	-	94	5
Miscellaneous													
Pentasiloxane, dodecamethyl-ARTEF	1.29 ± 0.032	0.05361	0.96 ± 0.031	0.77984	13.88	1164	0.07	147	-	✓	90.7	100	3
MSTFA ARTEF	0.91 ± 0.461	0.77600	0.33 ± 0.109	0.03575	18.34	1337	0.00	184	-	✓	80.0	94	3

Tetrasiloxane, decamethyl-ARTEF	2.23 ± 0.899	0.38459	2.74 ± 1.530	0.29463	18.75	1353	0.02	207	-	✓	81.5	78	3
Silane, trimethyl(octadecyloxy)-	↑	0.03379	↑	0.00009	34.50	2155	0.03	327	-	✓	89.0	39	3
Unknowns													
Unknown_8.45_984	1.53 ± 0.922	0.79797	0.50 ± 0.166	0.17888	8.45	984	0.10	134, 184, 214	-	-	-	94	0
Unknown_9.34_1011	0.68 ± 0.053	0.35157	0.33 ± 0.127	0.03900	9.34	1011	0.04	75, 144, 116	-	-	-	100	0
Unknown_12.33_1111	↑	0.39100	↓	0.00021	12.33	1111	0.01	89	-	-	-	33	0
Unknown_13.78_1160	2.07 ± 0.832	0.36240	0.47 ± 0.067	0.00536	13.78	1160	0.04	147, 117, 233	-	-	-	67	0
Unknown_14.90_1198	0.35 ± 0.246	0.06050	0.31 ± 0.053	0.00316	14.90	1198	0.04	200, 216, 189	-	-	-	89	0
Unknown_15.54_1223	2.67 ± 0.875	0.16692	0.44 ± 0.153	0.26365	15.54	1223	0.03	156	-	-	-	100	0
Unknown_16.97_1281	2.63 ± 0.930	0.18611	0.87 ± 0.053	0.71446	16.97	1281	0.02	124, 168	-	-	-	100	0
Unknown_17.60_1307	2.15 ± 0.452	0.16611	1.59 ± 0.442	0.34340	17.60	1307	0.08	91, 164, 193	-	-	-	94	0
Unknown_18.06_1325	19.77 ± 12.69	0.02611	1.97 ± 1.156	0.77133	18.06	1325	0.00	315, 330, 147	-	-	-	100	0
Unknown_19.26_1372	3.08 ± 0.729	0.03369	1.00 ± 0.295	0.94418	19.26	1372	0.03	83	-	-	-	100	0
Unknown_19.75_1394	33.06 ± 27.63	0.15809	2.83 ± 2.183	0.60550	19.75	1394	0.00	147, 241, 209, 288, 273	-	-	-	83	0
Unknown_20.08_1407	1.76 ± 0.392	0.24200	0.55 ± 0.054	0.27094	20.08	1407	0.01	100, 243	-	-	-	100	0
Unknown_20.21_1412	5.91 ± 4.446	0.23936	0.24 ± 0.058	0.04634	20.21	1412	0.04	70, 188	-	-	-	100	0
Unknown_20.46_1422	3.34 ± 1.791	0.13387	0.38 ± 0.052	0.00083	20.46	1422	0.02	244	-	-	-	100	0
Unknown_21.03_1445	1.22 ± 0.477	0.78746	0.43 ± 0.219	0.22219	21.03	1445	0.00	86, 103, 147, 247	-	-	-	94	0
Unknown_21.85_1463	3.73 ± 1.614	0.34219	0.90 ± 0.600	0.57340	21.85	1463	0.00	98, 172, 200	-	-	-	89	0
Unknown_21.74_1474	3.36 ± 0.912	0.03866	0.64 ± 0.060	0.08850	21.74	1474	0.00	68, 158, 260	-	-	-	100	0
Unknown_22.07_1488	2.69 ± 0.919	0.23180	0.62 ± 0.117	0.97698	22.07	1488	0.09	243, 100	-	-	-	100	0
Unknown_22.56_1509	1.82 ± 0.847	0.47589	0.30 ± 0.048	0.00037	22.56	1509	0.01	170	-	-	-	78	0
Unknown_23.92_1580	0.24 ± 0.098	0.20705	0.09 ± 0.033	0.00091	23.92	1580	0.02	82, 110, 200	-	-	-	89	0
Unknown_24.18_1591	↑	0.39100	3.49 ± 0.281	0.08328	24.18	1591	0.00	147, 169, 259	-	-	-	44	0
Unknown_24.62_1613	-	-	4.06 ± 2.664	0.29681	24.62	1613	0.01	117, 216, 283	-	-	-	22	0
Unknown_24.76_1620	5.70 ± 1.396	0.03259	0.37 ± 0.452	0.33847	24.76	1620	0.01	157, 275	-	-	-	78	0
Unknown_25.45_1655	2.38 ± 1.063	0.24560	0.36 ± 0.049	0.09751	25.45	1655	0.03	311, 208	-	-	-	100	0
Unknown_26.75_1719	0.51 ± 0.587	0.51176	0.41 ± 0.102	0.00673	26.75	1719	0.08	217, 103	-	-	-	72	0

Unknown_27.17_1742	1.064 ± 0.226	0.82640	0.22 ± 0.073	0.00496	27.17	1742	0.04	313, 147, 211	-	-	-	83	0
Unknown_27.44_1755	15.06 ± 12.03	0.20216	0.52 ± 0.123	0.05348	27.44	1755	0.03	117, 363	-	-	-	61	0
Unknown_27.50_1758	↓	0.03473	0.12 ± 0.151	0.21073	27.50	1758	0.01	430, 157	-	-	-	44	0
Unknown_28.21_1793	-	-	↓	0.01548	28.21	1793	0.01	204, 147	-	-	-	22	0
Unknown_28.93_1830	1.28 ± 0.124	0.28356	1.24 ± 0.082	0.04088	28.93	1830	0.04	147, 217, 117	-	-	-	100	0
Unknown_31.30_1958	7.05 ± 1.315	0.00742	5.96 ± 0.426	0.00899	31.30	1958	0.01	217, 299	-	-	-	89	0
Unknown_38.29_2413	1.12 ± 0.110	0.58905	0.34 ± 0.420	0.18873	38.29	2413	0.00	185, 281	-	-	-	89	0
Unknown_39.40_2493	0.90 ± 0.153	0.52590	0.47 ± 0.102	0.03460	39.40	2493	0.05	205, 117, 147, 313, 445	-	-	-	100	0
Unknown_47.75_3252	↓	0.02337	1.39 ± 0.199	0.36500	47.75	3252	0.00	98, 340, 396	-	-	-	100	0

Table heading definitions:

Compounds detected	Name of the compound and its derivatisation groups (TMS = trimethylsilyl).
Fold change (± SE)	Fold change in the average metabolite relative abundance from control to permethrin-exposed cells after 6 and 24 hours, ± standard error (SE) of the mean. ↑ = increased from below the limit of detection, ↓ = decreased to below the limit of detection, and no entry indicates the feature was undetectable in all samples at that time point.
P value	P values for 6 and 24 hours metabolite fold changes, calculated using a two-tailed Student's t test between the control and treatment groups per time point, of each metabolite feature using $\log_{10}(X + 1)$ transformed, normalised relative abundances. Data were considered non-normally distributed with unequal variances.
RT (min)	Average measured retention time in minutes.
RI	Average calculated retention index.
RI RSD (%)	Relative standard deviation of the average calculated retention index.
BP *m/z* (EI)	Deconvoluted base peak (or extracted ion) mass/es (EI = electron ionisation).
User library match	Indicates whether a compound was matched to a user-generated library of authentic metabolite standards.
NIST match	Indicates compounds confidently matched to NIST database with probability >80%.
NIST probability (%)	Average calculated NIST probability score for a NIST matched compound.
Detected in samples (%)	Proportion of samples (as a percentage) in which the compound was detected.
ID Score	Compound identification score based on the proposed identification scoring system outlined in Abbiss et al 2015: 7 = Match to authentic standard + RT ± 2.5% + confident NIST match 5 = Match to authentic standard + RT ± 2.5% 3 = Confident NIST match + RT ± 2.5% 1.5 = Confident NIST match 0.5 = Compound class match 0 = Unknown